NTNU
Norwegian University of
Science and Technology

Spectral Approximation of European and American Option Pricing Problems

Frida Marie Eidsæther Bruun

Master of Science in Physics and Mathematics
Submission date: June 2018
Supervisor: Espen Robstad Jakobsen, IMF

Norwegian University of Science and Technology
Department of Mathematical Sciences

Preface

This thesis represents the completion of my master's degree in the field of physics and mathematics at the Norwegian University of Science and Technology. It was written during the spring of 2018.

The thesis builds on a specialization project written during the fall of 2017, where the aim was for the author to gain knowledge about spectral methods and to apply spectral methods to a standard problem in option pricing. This thesis expands the project work for European options and concerns in addition the pricing of American options. In particular, the following work recovers spectral convergence for single-asset European options, which was not obtained in the project.

I wish to express gratitude to my supervisor Professor Espen Robstad Jakobsen, for productive discussions and constructive feedback throughout the development of this thesis. His guidance and advice have been of great help.

I would also like to thank Professor Anton Evgrafov for taking the time to discuss issues related to implementational work.

Trondheim, Norway *Frida Marie Bruun*

June, 2018

Abstract

In this thesis, properties of spectral methods applied to option pricing problems are investigated. The Legendre Galerkin method with numerical integration is applied to European and American option pricing problems under the Black-Scholes model. The method is coupled with an implicit time stepping technique for a full discretization. As a remedy for non-smooth payoff functions in option pricing, the method is combined with domain decomposition, where the domain is split at slope discontinuities. For the American pricing problem, an approach based on penalization is adapted. Numerical results indicate that the method provides spectral convergence for one-dimensional European options and fourth order convergence for two-dimensional European options and one-dimensional American options. Stability and convergence is proved for the numerical scheme of the one-dimensional European pricing problem.

Sammendrag

I denne avhandlingen undersøkes egenskapene til spektralmetoder anvendt på opsjonsprisingsproblemer. Legendre Galerkin-metoden med numerisk integrasjon blir anvendt på Europeiske og Amerikanske opsjonsprisingsproblemer under Black-Scholes-modellen. Metoden er koblet med en implisitt teknikk i tid for en fullstendig diskretisering. For å håndtere de ikke-glatte payoffunksjonene i opsjonsprising er metoden kombinert med domenenedbrytning hvor domenet er splittet i punkter der stigningstallet ikke er kontinuerlig. For det amerikanske opsjonsprisingsproblemet har det blitt anvendt en tilnærming basert på penalisering. Numeriske resultater indikerer at metoden gir spektral konvergens for endimensjonale Europeiske opsjoner og fjerde ordens konvergens for todimensjonale Europeiske opsjoner og endimensjonale Amerikanske opsjoner. Stabilitet og konvergens blir bevist for det diskretiserte endimensjonale Europeiske prisproblemet.

Table of Contents

Chapter 1

Introduction

Option pricing is an important problem in financial mathematics, due to the extensive use of options in financial markets. A wide variety of options are used in practice, among them European and American options. The European option is the simplest kind of options and an analytical formula exists for the European option price, which is the solution of the linear Black-Scholes equation. The price of an American option is the solution of an optimal stopping problem [3, 22], involving the Black-Scholes differential operator and a constraint on the value of the option. As opposed to European options, there is no known explicit analytical solution formula for the value of an American option [7][1]. Consequently, one must resort to numerical schemes to determine the solution of the American pricing problem.

The valuation of basket options is another subject of considerable significance in mathematical finance. This problem concerns options whose payoff is a weighted sum or average of prices of two or more underlying risky assets. Basket options are among the most popular contracts of the latest generation of exotic options. In general, it is difficult to price basket options explicitly since the joint distribution of the underlying basket asset price process are unknown due to multi-dimensionality [15]. Thus, some research have been devoted to the development of fast and accurate approximation techniques for basket option values.

Explicit pricing formulas for European options on non-dividend paying stocks were derived by Black and Scholes in their famous paper *The Pricing of Options and Corporate Liabilities* [8] in 1973. Following this, the research on the more complex valuation of American options has developed extensively. The valuation of American options began with McKean [21] in 1965, who transformed

[1] Solutions exist in some special cases, but they are unsuitable for application, due to complicated implementation [25].

the initial problem into a free boundary problem. Pursuing this, van Moerbeke studied the properties of the optimal stopping boundary [33]. This became the foundation of the work by Bensoussan [3] and Karatzas [22, 23] who showed that the price of the American option is a solution of the optimal stopping problem. An alternative technique of variational inequalities were developed by Bensoussan and Lions [5] in 1982. Guided by this effort, Jaillet, Lamberton and Lapeyre [20] worked on the same problem.

A standard approach for one-dimensional American-style options goes back to Brennan and Schwartz [9] and is based on discretizing a partial differential variational inequality spatially via a finite difference or finite element scheme, discretizing temporally via the fully implicit Euler scheme, and solving the resulting linear complementarity problem by a numerical algorithm, such as the Projected Successive Over-Relaxation (PSOR). Some other well known methods used for the problem consists in the binomial method introduced by Cox et al. [14] and the front-fixing method of Nielsen et al. [26]. An alternative to the PDE approach is to compute the option price with Monte-Carlo simulations. This technique is widely used in the financial industry, however the method requires considerable computational resources due to its slow convergence. In this thesis, we focus on the PDE approach to option pricing.

In 2003, Benth, Karlsen and Reikvam [7] provided a new formulation of the American option valuation problem. They derived a semilinear Black-Scholes type partial differential equation for the value of an American option and showed that there exists exactly one viscosity solution[2] of this equation, namely the American option value. A popular strategy for deriving this formulation is based on the penalty method, which will be used for numerical approximations of the American option value in this thesis. The penalty method benefits from being generalizable to multi-dimensional problems such as options on baskets.

For spatial discretization in the PDE approach, finite differences and finite elements have been used extensively over the last decades. These methods have achieved success in many cases due to their effectiveness and flexibility. However, these methods require a considerable number of grid points to obtain accurate solutions. Spectral methods is an attractive alternative, often providing a given accuracy with much less grid points (nodes) in less computing time. A Chebyshev collocation spectral method for the American pricing problem is presented by Song et al. [30] and Pindza [27] presents a rational spectral collocation method for European and American option pricing. Another related method is the spectral element method which combines the exponential convergence of spectral meth-

[2] For an appropriate definition of a viscosity solution.

ods with the geometric flexibility of finite element methods. A spectral element method for pricing European options is presented by Chen et al. [12].

In this thesis, we study the behaviour of a Legendre Galerkin spectral method with numerical integration for discretization of option pricing problems in the spatial direction. For smooth enough solutions, spectral methods are exponentially convergent in the number of degrees of freedom [31, 10, 17]. However, a main drawback for their direct applications to option pricing is that the initial conditions in the governing PDEs of the pricing problems are non-smooth with discontinuous second derivatives. Thus, the spectral approximations are reduced to low order accuracy, eliminating their advantage over simple finite difference methods.

Encouragingly, several ideas for overcoming this problem have been proposed in literature. One approach, proposed by Greenberg [19], is to regularize the initial condition. Another approach is to refine the number of nodes in the spectral approximation around the nonsmooth region of the initial condition. Tangman et al. [32] presents an approach which consists in dividing the set of nodes into two in the centre of the non-smooth region, thus clustering nodes at the singularity of the option price. In the following work, we will implement a version of this last approach through a domain decomposition method.

The thesis is organized as follows: An introduction to financial contracts are given in Chapter 2, followed by an introduction to the Black-Scholes model in Chapter 3 and an introduction to spectral methods in Chapter 4. Then the Legendre Galerkin method is applied to a single-asset European pricing problem in Chapter 5. In Chapter 6 we extend this problem to two dimensions and consider the valuation of a European option on a small basket of two underlying assets. An analysis of stability and convergence of the numerical scheme is provided for the one-dimensional European pricing problem in Chapter 7. After this, we study the method for valuation of American options using the penalty approach in Chapter 8. Finally, we conclude in Chapter 9 and propose ideas for further work related to these problems in Chapter 10. To the best of the authors knowledge, the Legendre Galerkin spectral method with numerical integration and domain decomposition applied to option pricing has not appeared in literature before.

Chapter 2

Financial Contracts and Options

Financial contracts are commonly used in finance, and many different contracts exist. One class of contracts is derivatives. A derivative is a contract that derives its value from the performance of an underlying asset. This asset may for instance be a stock, a bond or a commodity. Derivatives are widely used and offer investors the opportunity to tailor their trades to their investment needs. Some of the more common derivatives include forwards, futures, options, swaps, and variations of these.

An option is a contract sold by the option writer to an option holder. The option gives the holder the right to buy the underlying asset, or the option to sell it. The holder thus holds a right and not an obligation, while on the other side the writer holds a potential obligation. There are two basic versions of an option, the call option and the put option. A call option gives the holder the right to buy at a specified price, and the writer is obligated to sell at this price if the holder chooses to exercise the option. On the other hand, a put option gives the holder the option to sell at a specific price, and the writer is then obligated to buy. Furthermore, there exist different types of call and put options. The simplest ones being the European options.

Options are primarily used for speculation and hedging. A financial player looking to speculate may buy a call option if he or she expects a stock price to increase. If the stock's value increases beyond the specified price, the speculator will benefit from exercising the option. If however the stock price decreases, the speculator may choose to not exercise the option, and he or she has only lost the initial cost of buying the option. Another simple example may illustrate hedging. Say an oil company expects that the oil price will fall in the upcoming months. Then the company may buy a put option with oil as the underlying asset. The put option gives a guaranteed value of the company's oil. If the oil price rises, the company can choose to not exercise the option and sell the oil for a higher price. Hence the

option has provided the company with the security of limited risk.

Further relevant financial concepts for the remaining discussion are defined in the following:

Definition 1. Vanilla option

A normal call or put option that has no special or unusual features.

Definition 2. European option

An option that can only be exercised during a particular time period just before its expiration.

Definition 3. American option

An option that can be exercised at any time prior to and including its date of expiration.

Definition 4. Basket option

An option whose underlying is a weighted sum or average of different assets that have been grouped together in a basket.

Definition 5. Volatility

Volatility is a measure of how much the value of a stock or another financial instrument fluctuates or varies over a time period. Higher volatility means that the stock's value is more likely to be spread out over a larger range of values.

Definition 6. Risk-free interest rate

The risk-free interest rate is the theoretical rate of return on a risk-free investment. This rate represents the interest an investor would expect from an investment with zero risk over a specified period of time.

Definition 7. Strike price

The agreed-upon price at which an option can be exercised. The strike price for a call option is the price at which the security can be bought (up to the expiration date); the strike price for a put option is the price at which the security can be sold (up to the expiration date). The strike price is sometimes called the exercise price.

Definition 8. Arbitrage

The opportunity to make an instantaneous benefit without taking any risk.

In order to evaluate the market price of an option at a given time, we assume that the transactions have no cost and are instantaneous and that the market rules out arbitrage [2].

Chapter 3

The Black-Scholes Model

3.1 Single-Asset Black-Scholes Model

The theoretical value of an option is the estimated value of an option derived from a mathematical model. This value represents what the option should currently be worth using known input parameters such as the underlying asset price, the strike price and the time until expiration. There exist several different option pricing models that are used to determine the theoretical value of an option.

The Black-Scholes equation was the first widely used formula for option pricing. It is used to calculate the theoretical value of European-style options using current stock prices, expected dividends, the option's strike price, expected interest rates, time to expiration and expected volatility. Assumptions in the Black-Scholes model are the following:

- Constant volatility.
- Efficient markets.
- No dividends.
- Interest rates are constant and known.
- Log-normally distributed returns.
  The log-returns on the underlying stock are normally distributed.
- No commissions and transaction costs.
- Liquidity.

The Black-Scholes model assumes that markets are perfectly liquid and it is possible to purchase or sell any amount of stocks or options or their fractions at any given time.

In order to derive the Black-Scholes equation, let us first describe a simple model for the price of an asset, (see chapter 2 of [35]). We assume the changes in the asset price to be a Markov process. Since the absolute change in an asset price is not a useful quantity alone, we introduce the return, defined to be the change in the asset price divided by the asset's original value. Let S be the asset price at time t, then $^{dS}/_{S}$ is the return on the asset. The Black-Scholes model decomposes the return as a sum of a deterministic term μdt, called the drift, and a random term, assumed to be $\sigma\, dX$, modelling the price variations in response to external effects. More precisely, the risky asset is assumed to follow the stochastic differential equation

$$dS = S(\sigma dX + \mu dt), \tag{3.1}$$

where σ is the volatility measuring the standard deviation of the returns and X is a standard Brownian motion.

Suppose now that we have an option with value $V(S,t)$ depending on the asset price S and time t. Applying Itô's formula (see A.1) gives

$$dV = \sigma\, S\frac{\partial V}{\partial S}dX + \left(\mu S\frac{\partial V}{\partial S} + \frac{\partial V}{\partial t} + \frac{1}{2}\sigma^2 S^2\frac{\partial^2 V}{\partial S^2}\right)dt. \tag{3.2}$$

The equation describes the random walk followed by V.

Now, we construct a portfolio consisting of one option and an arbitrary number $-\Delta$ of the option's underlying asset. The portfolio's value is then

$$\Pi = V - \Delta S. \tag{3.3}$$

When moving one step in time, the change in value of the portfolio will be

$$d\Pi = dV - \Delta dS,$$

for a fixed Δ.

Combining (3.1), (3.2) and (3.3) we see that the portfolio value follows the random walk

$$d\Pi = \sigma\, S \left(\frac{\partial V}{\partial S} - \Delta \right) dX + \left(\mu S \frac{\partial V}{\partial S} + \frac{\partial V}{\partial t} + \frac{1}{2}\sigma^2 S^2 \frac{\partial^2 V}{\partial S^2} - \mu \Delta S \right) dt.$$

By choosing

$$\Delta = \frac{\partial V}{\partial S}, \tag{3.4}$$

we can remove the random contribution in the random walk above and obtain the following deterministic increment

$$d\Pi = \left(\frac{\partial V}{\partial t} + \frac{1}{2}\sigma^2 S^2 \frac{\partial^2 V}{\partial S^2} \right) dt.$$

We know that the return on a portfolio containing risk-free assets would increase in value by $r\Pi dt$ in one timestep dt, with r being the risk-free interest rate [35]. This implies

$$r\Pi dt = \left(\frac{\partial V}{\partial t} + \frac{1}{2}\sigma^2 S^2 \frac{\partial^2 V}{\partial S^2} \right) dt. \tag{3.5}$$

If we substitute the results from (3.3) and (3.4) into the above equation (3.5) we arrive at the **Black-Scholes equation**

$$\frac{\partial V(S,t)}{\partial t} + \frac{1}{2}\sigma^2 S^2 \frac{\partial^2 V(S,t)}{\partial S^2} + rS\frac{\partial V(S,t)}{\partial S} - rV(S,t) = 0, \tag{3.6}$$

which is valid for

$$S > 0, \qquad t \in [0, T),$$

where T is the time of expiration.

Remark 1 *The argument used above is presented in [35]. A slightly different argument is also commonly used in literature. It relies on showing that it is possible to simulate the option by a self-financed portfolio containing Δ shares of the underlying asset and Δ_0 shares of the risk-free asset. See for example [6].*

The Black-Scholes equation governs the price evolution of a European call or European put option under the Black-Scholes model. Appropriate boundary conditions and the value of the option at expi-

ration can be found by financial arguments. Due to the put-call parity, which describes the relationship between the price of European put options and European call options with the same underlying asset, strike price and expiration date, finding the price of a European put option determines the price of the corresponding call option, and vice versa. Only results for put options will be discussed in this thesis.

For a put option with strike price K, it is reasonable to exercise the option if $S < K$ at time of expiration T. In this case the option owner will make a benefit of $(K - S)$ by exercising the option and immediately buying the underlying asset. If $S \geq K$ the option's value is zero. Thus, assuming that there is no arbitrage, the value of the put option on the expiration date is

$$V_\circ = V(S,T) = \max(K - S, 0) = [K - S]^+. \tag{3.7}$$

This is a final condition for the Black-Scholes equation, commonly referred to as the *payoff function*.

Considering now the boundary conditions for a put option on a finite domain $(0, \bar{S})$. On the left hand side of the domain, in $S = 0$, the equation reduces to

$$\frac{\partial V}{\partial t} - rV = 0.$$

Hence, we can simply solve the equation in this point instead of imposing an additional boundary condition. When S tends to infinity the option will be worthless so the option price should be zero. Thus, a reasonable choice of boundary conditions are

$$\frac{\partial V}{\partial t}(0,t) = rV \tag{3.8a}$$

$$V(\bar{S},t) = 0. \tag{3.8b}$$

The naturally imposed condition in $S = 0$ corresponds to the exercise price corrected for a potential risk-free investment.

Another common choice for the boundary condition in $S = \bar{S}$ is

$$\frac{\partial V}{\partial S}(\bar{S},t) = 0, \tag{3.9}$$

which is a milder condition than the one in (3.8b).

Analytical solutions of the Black-Scholes equation are available and a derivation can be found in [35]. For a European put option with boundary conditions (3.8), Black-Scholes equation admits the solution

$$V(S,t) = Ke^{-r(T-t)}N(-d_2) - SN(-d_1),$$

where $N(\cdot)$ is the cumulative distribution function of a standard normal random variable.

Here

$$d_1 = \frac{\log(S/K) + (r + \frac{1}{2}\sigma^2)(T-t)}{\sigma\sqrt{T-t}}$$

and

$$d_2 = \frac{\log(S/K) + (r - \frac{1}{2}\sigma^2)(T-t)}{\sigma\sqrt{T-t}}.$$

3.2 Multi-Asset Black-Scholes Model

Consider now a portfolio consisting of one option and N underlying assets. Let S_i be the prices of the assets at time t, $i = 1, ..., N$ and each asset satisfies the usual dynamic

$$dS_i = S_i(\sigma_i dX_i + \mu_i dt), \qquad i = 1, ..., N. \tag{3.10}$$

The N processes X_i are standard Brownian motions which are correlated according to

$$dX_i dX_j = \rho_{ij} dt, \qquad i, j = 1, ..., N,$$

where ρ is given by

$$\rho = \begin{pmatrix} 1 & \rho_{12} & \rho_{13} & \cdots & \rho_{1N} \\ \rho_{12} & 1 & \rho_{23} & \cdots & \rho_{2N} \\ \rho_{13} & \rho_{23} & 1 & \cdots & \rho_{3N} \\ \vdots & \vdots & \vdots & \ddots & \vdots \\ \rho_{1N} & \rho_{2N} & \rho_{3N} & \cdots & 1, \end{pmatrix}$$

with $-1 \leq \rho_{ij} \leq 1$.

Hence we have

$$dS_i dS_j = \sigma_i \sigma_j S_i S_j \rho_{ij} dt, \qquad i, j = 1, ..., N. \tag{3.11}$$

Let the value of the option be $V = V(S_1, ..., S_N, t)$. Then the value Π of the portfolio is

$$\Pi = V - \sum_{i=1}^{N} \Delta_i S_i, \tag{3.12}$$

where $-\Delta_i$ are the shares of each asset in the portfolio.

When moving one step in time, the change in value of the portfolio will be

$$d\Pi = dV - \sum_{i=1}^{N} \Delta_i dS_i,$$

for fixed Δ_i's.

Applying Itô's formula (see A.1) for V gives

$$d\Pi = \left(\frac{\partial V}{\partial t} dt + \sum_{i=1}^{N} \frac{\partial V}{\partial S_i} dS_i + \sum_{i,j=1}^{N} \frac{1}{2} \frac{\partial^2 V}{\partial S_i \partial S_j} dS_i dS_j \right) - \sum_{i=1}^{N} \Delta_i dS_i. \tag{3.13}$$

As stated earlier, we know that the return on a portfolio containing risk-free assets satisfies $d\Pi = r\Pi dt$ [35]. Using this, together with equations (3.10), (3.11) and (3.12), the relation (3.13) becomes

$$\frac{\partial V}{\partial t}dt + \sum_{i=1}^{N} \frac{\partial V}{\partial S_i}(\sigma_i S_i dX_i + \mu_i S_i dt) + \sum_{i,j=1}^{N} \frac{1}{2}\frac{\partial^2 V}{\partial S_i \partial S_j}(\sigma_i \sigma_j S_i S_j \rho_{ij} dt)$$
$$- \sum_{i=1}^{N} \Delta_i(\sigma_i S_i dX_i + \mu_i S_i dt) = r\left(V - \sum_{i=1}^{N} \Delta_i S_i\right) dt.$$

Collecting dt and dX_i terms gives

$$\frac{\partial V}{\partial t} + \sum_{i=1}^{N} \frac{\partial V}{\partial S_i}\mu_i S_i + \sum_{i,j=1}^{N} \frac{1}{2}\frac{\partial^2 V}{\partial S_i \partial S_j}(\sigma_i \sigma_j \rho_{ij} S_i S_j) - \sum_{i=1}^{N} \Delta_i \mu_i S_i \tag{3.14}$$
$$- r\left(V - \sum_{i=1}^{N} \Delta_i S_i\right) = 0$$

and

$$\sum_{i=1}^{N} \left(\frac{\partial V}{\partial S_i}\sigma_i S_i - \Delta_i \sigma_i S_i\right) dX_i = 0.$$

From this last equation, and given the independence of the $X_i's$, we see that

$$\Delta_i = \frac{\partial V}{\partial S_i}, \qquad i = 1, ..., N.$$

Inserting this into (3.14) we arrive at the **multi-asset Black-Scholes equation**

$$\frac{\partial V}{\partial t} + \sum_{i,j=1}^{N} \frac{1}{2}\frac{\partial^2 V}{\partial S_i \partial S_j}(\sigma_i \sigma_j \rho_{ij} S_i S_j) + r\left(\sum_{i=1}^{N} \frac{\partial V}{\partial S_i} S_i - V\right) = 0.$$

The simple case where $N = 2$ and ρ equals the identity matrix will be discussed at a later time in this thesis. In this case, the multi-asset Black-Scholes equation reduces to

$$\frac{\partial V}{\partial t} + \frac{1}{2}\sigma_1^2 S_1^2 \frac{\partial^2 V}{\partial S_1^2} + \frac{1}{2}\sigma_2^2 S_2^2 \frac{\partial^2 V}{\partial S_2^2} + r\left(S_1 \frac{\partial V}{\partial S_1} + S_2 \frac{\partial V}{\partial S_2} - V\right) = 0, \tag{3.15}$$

valid for

$$S_1, S_2 > 0, \qquad t \in [0, T).$$

Some common choices for the final condition $V_\circ$ of a put option are

$$[K - \max(S_1, S_2)]^+ \tag{3.16a}$$

$$[K - \min(S_1, S_2)]^+ \tag{3.16b}$$

$$[K - \frac{1}{2}(S_1 + S_2)]^+, \tag{3.16c}$$

where K is the strike price.

The choice of boundary conditions will be discussed at a later time when deriving a numerical scheme for equation (3.15).

Chapter 4

Introduction to Spectral Methods

Spectral methods are a class of spatial discretizations for differential equations. Their formulation rely on the two key concepts of trial functions and test functions. The trial functions are used to approximate the solution while the test functions ensure that the approximate solution satisfies the differential equation and possible boundary conditions as closely as possible. The trial basis functions of spectral methods are infinitely differentiable, nearly orthogonal and global, as opposed to the local basis functions of finite-element methods.

There are three main types of spectral methods, the Galerkin, collocation and tau versions. These are distinguished by the choice of test functions. In the spectral Galerkin method, the test functions are chosen to be the same as the trial functions and the discretization is derived from a weak form of the problem. In the spectral collocation method the test functions are shifted Dirac delta-functions centred at the collocation points. Here, the differential equation is satisfied exactly at each collocation point. The tau approach is a modification to the Galerkin method, applicable to problems with non-periodic boundary conditions.

The spectral Galerkin method is also commonly combined with Gaussian quadrature formulas, often referred to as Galerkin with numerical integration. As mentioned earlier, Galerkin methods with numerical integration will be developed in this thesis.

Spectral methods are additionally distinguished by the particular choice of trial functions. The most common choices for the trial functions are trigonometric polynomials, Legendre polynomials and Chebyshev polynomials [13].

Chapter 5

The Single-Asset European Pricing Problem

5.1 A Legendre Galerkin Scheme with Numerical Integration

We would like to solve the Black-Scholes equation (3.6) with final condition (3.7) and the boundary condition proposed in (3.9). In $S = 0$ we simply solve the equation, corresponding to the boundary condition (3.8a). After deriving the weak formulation of the problem we will see that these conditions will be natural boundary conditions.

Originally, the above problem is defined on the infinite domain $(0, \infty)$. In order to solve the problem numerically, it is necessary to truncate the infinite domain into a finite domain $\Omega = (0, S_{\text{max}})$. The choice of S_{max} must be large enough so that the error introduced by imposing the corresponding boundary condition is sufficiently small.

In order to define the trial and test functions for a Legendre Galerkin scheme, consider the $N-$th degree orthogonal Legendre polynomial $L_N(x)$ on $[-1, 1]$. We choose the $N-1$ extrema of L_N, x_j for $j = 1, ..., N-1$ belonging to $(-1, 1)$, as our quadrature nodes along with the boundary points $x_0 = -1$ and $x_N = 1$. These are the Legendre Gauss-Lobatto nodes (see [13], Section 1.2.3). Based on these points we define the characteristic Lagrange polynomials

$$\psi_j(x) = \frac{1}{N(N+1)} \frac{(1-x^2)}{(x_j - x)} \frac{L'_N(x)}{L_N(x_j)}, \qquad j = 0, ..., N,$$

or equivalently

$$\psi_j(x) = \prod_{i=0, i\neq j}^{N} \frac{(x - x_i)}{(x_j - x_i)}, \qquad j = 0, ..., N. \tag{5.1}$$

These are $N-$th degree polynomials which satisfy

$$\psi_j(x_k) = \delta_{jk}, \qquad j, k = 0, ..., N.$$

We choose these as our trial and test functions and seek a solution taking the form

$$V^N(x, t) = \sum_{i=0}^{N} V_i(t)\psi_i(x). \tag{5.2}$$

Now we derive the weak formulation of the Black-Scholes equation (3.6). Multiplying the equation with any of the test functions and integrating over the domain gives

$$\begin{aligned} \int_\Omega \frac{\partial V}{\partial t}\psi_j dS + \frac{1}{2}\sigma^2 \int_\Omega S^2 \frac{\partial^2 V}{\partial S^2}\psi_j dS + r\int_\Omega S\frac{\partial V}{\partial S}\psi_j dS - r\int_\Omega V\psi_j dS = 0, \\ j = 0, ..., N. \end{aligned} \tag{5.3}$$

Integration by parts of the second term yields

$$\begin{aligned} \frac{1}{2}\sigma^2 \int_\Omega S^2 \frac{\partial^2 V}{\partial S^2}\psi_j dS &= \frac{1}{2}\sigma^2 S^2 \frac{\partial V}{\partial S}\psi_j \Big|_{S=0}^{S=S_{\max}} - \sigma^2 \int_\Omega S\frac{\partial V}{\partial S}\psi_j dS \\ -\frac{1}{2}\sigma^2 \int_\Omega S^2 \frac{\partial V}{\partial S}\frac{d\psi_j}{dS} dS &= -\sigma^2 \int_\Omega S\frac{\partial V}{\partial S}\psi_j dS - \frac{1}{2}\sigma^2 \int_\Omega S^2 \frac{\partial V}{\partial S}\frac{d\psi_j}{dS} dS, \end{aligned}$$

for our choice of boundary conditions. Inserting this in (5.3) above gives

$$\begin{aligned} \int_\Omega \frac{\partial V}{\partial t}\psi_j dS - (\sigma^2 - r)\int_\Omega S\frac{\partial V}{\partial S}\psi_j dS - \frac{1}{2}\sigma^2 \int_\Omega S^2 \frac{\partial V}{\partial S}\frac{d\psi_j}{dS} dS - r\int_\Omega V\psi_j dS = 0, \\ j = 0, ..., N. \end{aligned}$$

Define

$$\begin{aligned} (V(t), \psi) &= \int_\Omega V(t)\psi dS \\ a(V, \psi) &= -(\sigma^2 - r)\int_\Omega S\frac{\partial V}{\partial S}\psi dS - \frac{1}{2}\sigma^2 \int_\Omega S^2 \frac{\partial V}{\partial S}\frac{d\psi}{dS} dS - r\int_\Omega V\psi dS, \end{aligned} \tag{5.4}$$

then we seek a solution $V(t)$ of the weak formulation[1]:

$$\begin{cases} \text{For } t \in (0,T) \text{ a.e., find } V(t) \text{ such that} \\ \frac{d}{dt}(V(t),\psi_j) + a(V(t),\psi_j) = 0, \quad j = 0,...,N \\ V|_{t=T} = V_\circ. \end{cases} \tag{5.5}$$

Since our quadrature nodes are distributed over the interval $\hat{\Omega} = (-1,1)$, we perform a transformation to this reference domain. The mapping used for S is

$$S(\xi) = \frac{S_{\max} - S_{\min}}{2}(\xi + 1) + S_{\min}, \qquad \frac{\partial S}{\partial \xi} = \frac{S_{\max} - S_{\min}}{2}. \tag{5.6}$$

Since $S_{\min} = 0$ this becomes

$$S(\xi) = \frac{S_{\max}}{2}(\xi + 1), \qquad \frac{\partial S}{\partial \xi} = \frac{S_{\max}}{2}, \tag{5.7}$$

and in particular, the Jacobian is given by $J = {}^{S_{\max}}\!/_2$.

With this choice of mapping the integral conditions can be written as

$$J\int_{\hat{\Omega}} \frac{\partial V}{\partial t}\psi_j d\xi - \frac{1}{J}\frac{\sigma^2}{2}\int_{\hat{\Omega}} S^2(\xi)\frac{\partial V}{\partial \xi}\frac{d\psi_j}{d\xi}d\xi - (\sigma^2 - r)\int_{\hat{\Omega}} S(\xi)\frac{\partial V}{\partial \xi}\psi_j d\xi - rJ\int_{\hat{\Omega}} V\psi_j d\xi = 0,$$
$$j = 0,...,N.$$

These are the equations we also ask the approximate solution V^N to satisfy. Replacing V with V^N yields the numerical scheme

$$\begin{aligned} &J\int_{\hat{\Omega}} \frac{\partial V^N}{\partial t}\psi_j d\xi - \frac{1}{J}\frac{\sigma^2}{2}\int_{\hat{\Omega}} S^2(\xi)\frac{\partial V^N}{\partial \xi}\frac{d\psi_j}{d\xi}d\xi \\ &- (\sigma^2 - r)\int_{\hat{\Omega}} S(\xi)\frac{\partial V^N}{\partial \xi}\psi_j d\xi - rJ\int_{\hat{\Omega}} V^N\psi_j d\xi = 0, \qquad j = 0,...,N. \end{aligned} \tag{5.8}$$

In order to evaluate the above integrals we resort to numerical integration and choose the Gauss-Lobatto quadrature (see [13], Section 2.2.3) based on the quadrature nodes found earlier. For weights

[1] A rigorous weak formulation is presented in Chapter 7.

given by

$$w_j = \frac{2}{N(N+1)} \frac{1}{(L_N(x_j))^2}, \qquad j = 0, ..., N,$$

we have the quadrature formula

$$\int_{-1}^{1} p(x)dx \approx \sum_{j=0}^{N} w_j p(x_j). \tag{5.9}$$

This formula is exact for polynomials of degree less or equal to $2N - 1$. Applying it to the integrals in equation (5.8) lets us obtain the following scheme

$$\begin{aligned} &J \sum_{k=0}^{N} w_k \left(\frac{\partial V^N}{\partial t} \psi_j \right)(\xi_k) - \frac{1}{J} \frac{\sigma^2}{2} \sum_{k=0}^{N} w_k \left(S^2 \frac{\partial V^N}{\partial \xi} \frac{d\psi_j}{d\xi} \right)(\xi_k) \\ &-(\sigma^2 - r) \sum_{k=0}^{N} w_k \left(S \frac{\partial V^N}{\partial \xi} \psi_j \right)(\xi_k) - rJ \sum_{k=0}^{N} w_k \left(V^N \psi_j \right)(\xi_k) = 0, \\ &\qquad\qquad\qquad\qquad\qquad\qquad\qquad\qquad\qquad\qquad j = 0, ..., N. \end{aligned} \tag{5.10}$$

Unfortunately, we can now observe that the terms inside the sums are polynomials of degree $2N$, hence our quadrature formula is not exact. However, this will only introduce a small error and we proceed with this approach.

5.2 The Scheme as a System of Algebraic Equations

The scheme (5.10) can be reformulated as a system $M\dot{V} + AV = 0$ of algebraic equations by inserting the expansion (5.2) for V^N. This gives the following system

$$\sum_{l=0}^{N} M_{jl} \frac{dV_l}{dt} + \sum_{l=0}^{N} A_{jl} V_l = 0, \qquad j = 0, ..., N,$$

where V_l are the unknowns and the matrix entries are given by

$$M_{jl} = J \sum_{k=0}^{N} w_k \psi_l(\xi_k) \psi_j(\xi_k),$$

and

$$A_{jl} = -\frac{1}{J}\frac{\sigma^2}{2}\sum_{k=0}^{N} w_k \left(S^2 \frac{d\psi_l}{d\xi}\frac{d\psi_j}{d\xi} \right)(\xi_k) - (\sigma^2 - r)\sum_{k=0}^{N} w_k \left(S\frac{d\psi_l}{d\xi}\psi_j \right)(\xi_k) - rJ\sum_{k=0}^{N} w_k \left(\psi_l \psi_j\right)(\xi_k).$$

Using the properties of the Lagrange polynomials ψ_j and ψ_l we can simplify the expressions for M_{jl} and A_{jl} to

$$M_{jl} = J w_j \delta_{jl},$$

and

$$A_{jl} = -\frac{1}{J}\frac{\sigma^2}{2}\sum_{k=0}^{N} w_k \left(S^2 \frac{d\psi_l}{d\xi}\frac{d\psi_j}{d\xi} \right)(\xi_k) - (\sigma^2 - r) w_j \left(S\frac{d\psi_l}{d\xi} \right)(\xi_j) - rJ w_j \delta_{jl}.$$

We can now find a solution numerically by implementing an appropriate solver for the linear system $M\dot{V}(t) + AV(t) = 0$ described above. This is a system of ordinary differential equations which can be solved using a two-level time-stepping method with a splitting parameter θ. This method consists in a discretization of the time derivative and a replacement of the other terms by a linear combination of the values at two consecutive timesteps, depending on the choice of θ, with $\theta \in [0, 1]$. For a right hand side equal to zero, the method reads

$$M\frac{V^{i+1} - V^i}{\Delta t} + A[\theta V^{i+1} + (1 - \theta)V^i] = 0, \tag{5.11}$$

where $i = 0, 1, ...$ denotes the discretization timestep, $\Delta t = t^{i+1} - t^i$ and V^i indicates that V is evaluated at time t^i. An implicit technique is obtained with $\theta \in [1/2, 1]$. The two cases $\theta = 1$ and $\theta = 1/2$ corresponds to the first order backward Euler method and second order Crank-Nicolson method, respectively.

To evaluate the accuracy of the method we will study the convergence of the numerical solution. This requires measuring the difference between the exact solution and the numerical approximation and in order to do this we define the following norm through approximation of the L^2-norm:

$$\begin{aligned} \|V_{\text{exact}}(\cdot,t) - V^N(\cdot,t)\| &= \left(\int_{-1}^{1} |V_{\text{exact}}(\xi,t) - V^N(\xi,t)|^2 d\xi\right)^{1/2} \\ &\approx \left(\sum_{j=0}^{N} w_j |V_{\text{exact}}(\xi_j,t) - V^N(\xi_j,t)|^2\right)^{1/2} = \|V_{\text{exact}}(\cdot,t) - V^N(\cdot,t)\|_{\tilde{L}^2}, \end{aligned} \tag{5.12}$$

with t being some fixed time, and w_j and ξ_j being the Legendre Gauss-Lobatto weights and nodes, respectively. This norm is based on the Gauss-Lobatto quadrature and is thus a suitable choice of norm in our case. It will be denoted by $||\cdot||_{\tilde{L}^2}$ throughout this thesis.

5.3 Introduction to Domain Decomposition

Due to the non-smooth payoff function of the option pricing problem, it is necessary to increase the number of nodes in the vicinity of the region of rapid change in order to restore spectral convergence. Here, domain decomposition is proposed as a remedy, based on the research by F. Youbi, E. Pindza and E. Maré [36]. Their paper shows that domain decomposition attains the best spatial convergence rate for the European option pricing problem compared to the methods of grid stretching and discontinuity inclusion.

In spectral domain decomposition, the domain is divided into subdomains and the solution is approximated in each subdomain. Let us split the domain D into N_D intervals,

$$D_1 = (x^{(0)}, x^{(1)}),\ D_2 = (x^{(1)}, x^{(2)}), ...,\ D_{N_D} = (x^{(N_D-1)}, x^{(N_D)}),$$

with $x^{(0)} = 0$ and $x^{(N_D)} = S_{\text{max}}$. The N_D subdomains cover D as

$$D = \bigcup_{l=1}^{N_D} D_l,$$

where each subdomain has its own set of basis functions and expansion coefficients

$$u^{(l)}(x,t) = \sum_{k=0}^{N_l} \tilde{u}_k^{(l)}(t)\phi_k^{(l)}(x), \qquad x \in D_l, \qquad l = 1, ..., N_D.$$

In general, the different subdomains can touch or overlap each other. Here we consider only the case of nonoverlapping intervals. In order for each function $u^{(l)}$ to fit together and form a smooth solution over the full domain, the following conditions must be satisfied:

On the intersection surface of two touching subdomains D_l and D_v we require

$$\begin{cases} u^{(l)}(x) = u^{(v)}(x) \\ \frac{\partial u^{(l)}}{\partial n}(x) = -\frac{\partial u^{(v)}}{\partial n}(x), \qquad x \in \partial D_l \cap \partial D_v, \end{cases}$$

where n is the outer unit normal direction. This ensures a continuous solution with continuous first derivatives across the interface.

Since the Legendre Gauss-Lobatto nodes lie closer together near the end-points of a domain, domain decomposition will lead to a higher distribution of nodes near the interface of each subdomain. Thus, a natural choice for our problem is to have two subdomains with the transition point at the strike price K, where the initial condition is not differentiable. In the following we consider domain decomposition with two subdomains. The method can easily be extended to cases with more than two subdomains.

Let the interface be denoted by $\Gamma = \partial D_1 \cap \partial D_2$ and let $\tilde{N}$ be the total number of nodes in D. We write $\tilde{N} = \tilde{N_1} + \tilde{N_2} + \tilde{N_\Gamma}$ with $\tilde{N_\Gamma}$ being the number of nodes on the interface Γ. Denote the vectors of unknowns in the spectral approximation by $\mathbf{u}_1, \mathbf{u}_2$ and $\mathbf{u}_\Gamma$ with $\tilde{N_1}, \tilde{N_2}$ and $\tilde{N_\Gamma}$ being their lengths, respectively. Let $\phi_j^{(i)}$ be the basis functions associated with the nodes lying in D_i and $\phi_r^{(\Gamma)}$ be the basis functions associated with the nodes lying on Γ.

Furthermore, define for $i = 1, 2$

$$\begin{aligned} (M_{ii})_{lj} &= \begin{cases} \left(\psi_j^{(i)}, \psi_l^{(i)}\right)_{D_i}, & l = j = 1, ..., \tilde{N}_i \\ 0, & \text{otherwise} \end{cases} \\ (M_{\Gamma\Gamma})_{sr} &= \begin{cases} \left(\psi_r^{(\Gamma)}, \psi_s^{(\Gamma)}\right)_{D_1} + \left(\psi_r^{(\Gamma)}, \psi_s^{(\Gamma)}\right)_{D_2}, & s = r = 1, ..., \tilde{N_\Gamma}, \\ 0, & \text{otherwise} \end{cases} \end{aligned} \tag{5.13}$$

and

$$
\begin{aligned}
(A_{ii})_{lj} &= a_i\left(\psi_j^{(i)}, \psi_l^{(i)}\right), \quad l,j = 1,...,\tilde{N}_i \\
(A_{i\Gamma})_{lr} &= a_i\left(\psi_r^{(\Gamma)}, \psi_l^{(i)}\right), \quad l = 1,...,\tilde{N}_i, r = 1,...,\tilde{N}_\Gamma \\
(A_{\Gamma i})_{rl} &= a_i\left(\psi_l^{(i)}, \psi_r^{(\Gamma)}\right), \quad l = 1,...,\tilde{N}_i, r = 1,...,\tilde{N}_\Gamma \\
(A_{\Gamma\Gamma})_{sr} &= a_1\left(\psi_r^{(\Gamma)}, \psi_s^{(\Gamma)}\right) + a_2\left(\psi_r^{(\Gamma)}, \psi_s^{(\Gamma)}\right), \quad s,r = 1,...,\tilde{N}_\Gamma,
\end{aligned}
\tag{5.14}
$$

where $a_i(\cdot,\cdot)$ is the restriction of the bilinear form $a(\cdot,\cdot)$ to subdomain D_i. Our problem can then be written in the algebraic form $M\dot{V} + AV = 0$ and presented in block form as

$$
\begin{pmatrix} M_{11} & 0 & 0 \\ 0 & M_{22} & 0 \\ 0 & 0 & M_{\Gamma\Gamma} \end{pmatrix}
\begin{pmatrix} \dot{\mathbf{u}}_1 \\ \dot{\mathbf{u}}_2 \\ \dot{\mathbf{u}}_\Gamma \end{pmatrix}
+
\begin{pmatrix} A_{11} & 0 & A_{1\Gamma} \\ 0 & A_{22} & A_{2\Gamma} \\ A_{\Gamma 1} & A_{\Gamma 2} & A_{\Gamma\Gamma} \end{pmatrix}
\begin{pmatrix} \mathbf{u}_1 \\ \mathbf{u}_2 \\ \mathbf{u}_\Gamma \end{pmatrix}
=
\begin{pmatrix} \mathbf{0}_1 \\ \mathbf{0}_2 \\ \mathbf{0}_\Gamma \end{pmatrix},
\tag{5.15}
$$

where $\mathbf{0}_k$ is the zero vector of length $\tilde{N}_k$ for $k = 1, 2, \Gamma$.

The blocks A_{12} and A_{21} are zero under the assumption that the nodes in D_1 and D_2 are not directly coupled except through nodes on the interface Γ [11].

The implementation of domain decomposition is also expected to reduce the computation time significantly if one makes use of parallel processing. The method is suitable for parallel computing in the case of independent problems on each subdomain, which is in fact the case for the option pricing problems considered in this thesis. Additional material on domain decomposition methods can be found in [29].

5.4 A Numerical Scheme with Domain Decomposition

Here, we choose to divide the domain $\Omega = (0, S_{\text{max}})$ into three subdomains

$$
\Omega_1 = (0, K), \quad \Omega_2 = (K, 2K), \quad \Omega_3 = (2K, S_{\text{max}}).
$$

This choice is motivated by the properties of the solution. The solution changes the most near K and changes slowly when $S > 2K$. Furthermore, it is desirable to localize a high number of nodes close to K and with two equally large domains at each side of K we obtain a steady distribution of points

around K. In $S > 2K$, less nodes are needed and with one domain covering this area it is possible to reduce the density of nodes here.

We indicate by $V^{(i)}$ the restriction of the solution V of (5.5) to Ω_i, $i = 1, 2, 3$ and define

$$\begin{aligned}
\left(V^{(i)}, \psi^{(i)}\right)_{\Omega_i} &= \int_{\Omega_i} V^{(i)}(t)\psi^{(i)} dS \\
a_i\left(V^{(i)}, \psi^{(i)}\right) &= \frac{1}{2}\sigma^2 S^2 \frac{\partial V^{(i)}}{\partial S}\psi^{(i)}\Big|_{S=S_{\min}(\Omega_i)}^{S=S_{\max}(\Omega_i)} - (\sigma^2 - r)\int_{\Omega_i} S\frac{\partial V^{(i)}}{\partial S}\psi^{(i)} dS \\
&\quad - \frac{1}{2}\sigma^2 \int_{\Omega_i} S^2 \frac{\partial V^{(i)}}{\partial S}\frac{d\psi^{(i)}}{dS} dS - r\int_{\Omega_i} V^{(i)}\psi^{(i)} dS,
\end{aligned} \tag{5.16}$$

where $\psi^{(i)}$ are the test functions associated with the nodes lying in the closed subdomain $\overline{\Omega}_i$.

On each subdomain we choose as test functions the N_i-th degree polynomials defined in (5.1). Then the problem in (5.5) admits the following equivalent three-domain formulation, for $t \in (0, T)$ a.e.:

$$\begin{cases} \frac{d}{dt}\left(u^{(i)}(t), \psi_j^{(i)}\right)_{\Omega_i} + a_i\left(u^{(i)}(t), \psi_j^{(i)}\right) = 0 \\ V^{(i)}(0) = V_{\circ|\Omega_i}, \quad j = 0, ..., N_i, \quad i = 1, 2, 3, \end{cases} \tag{5.17}$$

where in addition the following interface conditions has to be satisfied

$$\begin{cases} V^{(1)}(S) = V^{(2)}(S) \\ \frac{\partial V^{(1)}}{\partial n}(S) = -\frac{\partial V^{(2)}}{\partial n}(S), \qquad S \in \partial\Omega_1 \cap \partial\Omega_2 \\ V^{(2)}(S) = V^{(3)}(S) \\ \frac{\partial V^{(2)}}{\partial n}(S) = -\frac{\partial V^{(3)}}{\partial n}(S), \qquad S \in \partial\Omega_2 \cap \partial\Omega_3, \end{cases} \tag{5.18}$$

to obtain a solution in C^1.

We now map each subdomain to the reference domain $\hat{\Omega} = (-1, 1)$ through the linear transformation

$$S(\xi) = \begin{cases} \frac{K}{2}(\xi+1), & S \in \Omega_1 \\ \frac{K}{2}(\xi+1) + K, & S \in \Omega_2 \\ \frac{S_{\max}-2K}{2}(\xi+1) + 2K, & S \in \Omega_3, \end{cases}$$

calculated from the transformation shown in (5.7).

The Jacobian of each element, $J = \frac{\partial S}{\partial \xi}$, is then given by

$$J = \begin{cases} \frac{K}{2}, & S \in \Omega_1 \\ \frac{K}{2}, & S \in \Omega_2 \\ \frac{S_{\max}-2K}{2}, & S \in \Omega_3. \end{cases}$$

Denoting $J_i = J_{|\Omega_i}$, this gives the new formulation of (5.16)

$$\begin{aligned} \left(V^{(i)}, \psi^{(i)}\right)_{\hat{\Omega}} &= J_i \int_{\hat{\Omega}} V^{(i)}(t)\psi^{(i)} d\xi \\ a_i\left(V^{(i)}, \psi^{(i)}\right) &= \frac{1}{2J_i}\sigma^2 S^2(\xi)\frac{\partial V^{(i)}}{\partial \xi}\psi^{(i)}\Big|_{S=S_{\min}(\Omega_i)}^{S=S_{\max}(\Omega_i)} - (\sigma^2 - r)\int_{\hat{\Omega}} S(\xi)\frac{\partial V^{(i)}}{\partial \xi}\psi^{(i)} d\xi \\ &\quad -\frac{1}{2J_i}\sigma^2 \int_{\hat{\Omega}} S^2(\xi)\frac{\partial V^{(i)}}{\partial \xi}\frac{d\psi^{(i)}}{d\xi} d\xi - rJ_i \int_{\hat{\Omega}} V^{(i)}\psi^{(i)} d\xi. \end{aligned}$$

Upon denoting by $V^{N,(i)}$ the restriction of V^N to Ω_i, the approximate solution V^N is sought in the form

$$V^{N,(i)}(x,t) = \sum_{k=0}^{N_i} V_k^{(i)}(t)\psi_k^{(i)}(x), \qquad x \in \Omega_i, \qquad i = 1,2,3. \tag{5.19}$$

Enforcing the conditions in (5.17) and (5.18) on the approximate solution V^N lets us obtain the numerical scheme

$$J_1 \int_{\hat{\Omega}} \frac{dV^{N,(1)}}{dt}(t)\psi_j^{(1)} d\xi + \frac{1}{2J_1}\sigma^2 K^2 \frac{\partial V^{N,(1)}}{\partial \xi}\psi_j^{(1)}(K)$$
$$- (\sigma^2 - r)\int_{\hat{\Omega}} S(\xi)\frac{\partial V^{N,(1)}}{\partial \xi}\psi_j^{(1)} d\xi - \frac{1}{2J_1}\sigma^2 \int_{\hat{\Omega}} S^2(\xi)\frac{\partial V^{N,(1)}}{\partial \xi}\frac{d\psi_j^{(1)}}{d\xi} d\xi$$
$$- rJ_1 \int_{\hat{\Omega}} V^{N,(1)}\psi_j^{(1)} d\xi = 0, \qquad \xi \in \hat{\Omega}, \quad j = 0, ..., N_1$$

$$J_2 \int_{\hat{\Omega}} \frac{dV^{N,(2)}}{dt}(t)\psi_j^{(2)} d\xi + \frac{1}{2J_2}\sigma^2 (2K)^2 \frac{\partial V^{N,(2)}}{\partial \xi}\psi_j^{(2)}(2K)$$
$$- \frac{1}{2J_2}\sigma^2 K^2 \frac{\partial V^{N,(2)}}{\partial \xi}\psi_j^{(2)}(K) - (\sigma^2 - r)\int_{\hat{\Omega}} S(\xi)\frac{\partial V^{N,(2)}}{\partial \xi}\psi_j^{(2)} d\xi$$
$$- \frac{1}{2J_2}\sigma^2 \int_{\hat{\Omega}} S^2(\xi)\frac{\partial V^{N,(2)}}{\partial \xi}\frac{d\psi_j^{(2)}}{d\xi} d\xi - rJ_2 \int_{\hat{\Omega}} V^{N,(2)}\psi_j^{(2)} d\xi = 0,$$
$$\xi \in \hat{\Omega}, \quad j = 0, ..., N_2$$

$$J_3 \int_{\hat{\Omega}} \frac{dV^{N,(3)}}{dt}(t)\psi_j^{(3)} d\xi - \frac{1}{2J_3}\sigma^2 (2K)^2 \frac{\partial V^{N,(3)}}{\partial \xi}\psi_j^{(3)}(2K)$$
$$- (\sigma^2 - r)\int_{\hat{\Omega}} S(\xi)\frac{\partial V^{N,(3)}}{\partial \xi}\psi_j^{(3)} d\xi - \frac{1}{2J_3}\sigma^2 \int_{\hat{\Omega}} S^2(\xi)\frac{\partial V^{N,(3)}}{\partial \xi}\frac{d\psi_j^{(3)}}{d\xi} d\xi$$
$$- rJ_3 \int_{\hat{\Omega}} V^{N,(3)}\psi_j^{(3)} d\xi = 0, \qquad \xi \in \hat{\Omega}, \quad j = 0, ..., N_3,$$

where the boundary condition (3.9) have been incorporated in a weak manner.

After applying the Gauss-Lobatto quadrature formula (5.9) we arrive at the scheme

$$J_1 \sum_{k=0}^{N} w_k \left(\frac{dV}{dt}^{N,(1)}(t)\psi_j^{(1)} \right)(\xi_k) + \frac{1}{2J_1}\sigma^2 K^2 \frac{\partial V^{N,(1)}}{\partial \xi}\psi_j^{(1)}(1)$$
$$- (\sigma^2 - r) \sum_{k=0}^{N} w_k \left(S\frac{\partial V^{N,(1)}}{\partial \xi}\psi_j^{(1)} \right)(\xi_k) - \frac{1}{2J_1}\sigma^2 \sum_{k=0}^{N} w_k \left(S^2 \frac{\partial V^{N,(1)}}{\partial \xi}\frac{d\psi_j^{(1)}}{d\xi} \right)(\xi_k)$$
$$- rJ_1 \sum_{k=0}^{N} w_k \left(V^{N,(1)}\psi_j^{(1)} \right)(\xi_k) = 0, \quad \xi \in \hat{\Omega}, \quad j = 0, ..., N_1$$

$$J_2 \sum_{k=0}^{N} w_k \left(\frac{dV}{dt}^{N,(2)}(t)\psi_j^{(2)} \right)(\xi_k) + \frac{1}{2J_2}\sigma^2 (2K)^2 \frac{\partial V^{N,(2)}}{\partial \xi}\psi_j^{(2)}(1)$$
$$- \frac{1}{2J_2}\sigma^2 K^2 \frac{\partial V^{N,(2)}}{\partial \xi}\psi_j^{(2)}(-1) - (\sigma^2 - r) \sum_{k=0}^{N} w_k \left(S\frac{\partial V^{N,(2)}}{\partial \xi}\psi_j^{(2)} \right)(\xi_k)$$
$$- \frac{1}{2J_2}\sigma^2 \sum_{k=0}^{N} w_k \left(S^2 \frac{\partial V^{N,(2)}}{\partial \xi}\frac{d\psi_j^{(2)}}{d\xi} \right)(\xi_k) - rJ_2 \sum_{k=0}^{N} w_k \left(V^{N,(2)}\psi_j^{(2)} \right)(\xi_k) = 0,$$
$$\xi \in \hat{\Omega}, \quad j = 0, ..., N_2$$

$$J_3 \sum_{k=0}^{N} w_k \left(\frac{dV}{dt}^{N,(3)}\psi_j^{(3)} \right)(\xi_k) - \frac{1}{2J_3}\sigma^2 (2K)^2 \frac{\partial V^{N,(3)}}{\partial \xi}\psi_j^{(3)}(-1)$$
$$- (\sigma^2 - r) \sum_{k=0}^{N} w_k \left(S\frac{\partial V^{N,(3)}}{\partial \xi}\psi_j^{(3)} \right)(\xi_k) - \frac{1}{2J_3}\sigma^2 \sum_{k=0}^{N} w_k \left(S^2 \frac{\partial V^{N,(3)}}{\partial \xi}\frac{d\psi_j^{(3)}}{d\xi} \right)(\xi_k)$$
$$- rJ_3 \sum_{k=0}^{N} w_k \left(V^{N,(3)}\psi_j^{(3)} \right)(\xi_k) = 0, \quad \xi \in \hat{\Omega}, \quad j = 0, ..., N_3,$$

where ξ_k and w_k are the Legendre Gauss-Lobatto nodes and weights, respectively.

After inserting the expansions (5.19) for $V^{N,(i)}, i = 1, 2, 3$ and incorporating the interface conditions in (5.18) we can rephrase this scheme as a system $M\dot{V} + AV = 0$ of algebraic equations which can be written in the form (5.15) extended to three domains. The system can then be solved using the two-level time-stepping method presented in (5.11).

5.5 Numerical Solutions for a Single-Asset European Put Option

Results from solving Black-Scholes equation (3.6) for a European vanilla put option with payoff function (3.7) and boundary condition (3.9) are presented in the following. For temporal discretization, Crank-Nicolson timestepping has been used and results are shown for the final timestep.

The choice of parameters used in the numerical experiments is shown in Table 5.1.

Parameter	Value
r	0.05
σ	0.3
K	10
T	0.5
S_{max}	60

Table 5.1: Parameter values for the European put option.

The results presented here are mainly based on the Legendre Galerkin method with numerical integration and domain decomposition. In the convergence plot, this method is compared to the method without domain decomposition. The domain decomposition has been implemented with three subdomains, $\Omega_1 = (0, K), \Omega_2 = (K, 2K), \Omega_3 = (2K, S_{\text{max}})$. The distribution of the nodes for $N_i = 7$ on each subdomain $\Omega_i, i = 1, 2, 3$, is shown in Figure 5.1. When domain decomposition is not used, N is the polynomial degree. In the method with domain decomposition, we let N denote the sum of polynomial degrees on each subdomain, i.e. $N = \sum_i N_i$, $i = 1, 2, 3$. With this notation, $N + 1$ is the total number of nodes in both methods. In the following, we take N_i to be equal on each subdomain. Thus N corresponds to $3N_i$.

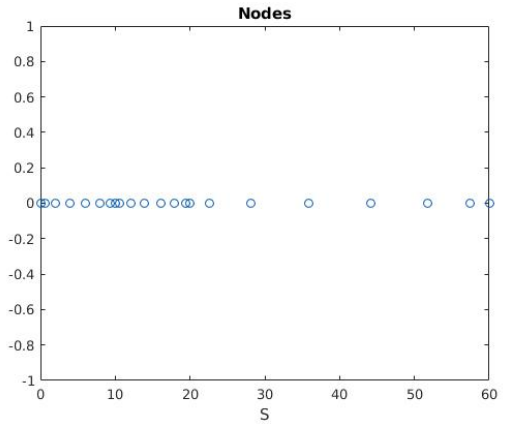

(a) Distribution of the nodes along the S-axis.

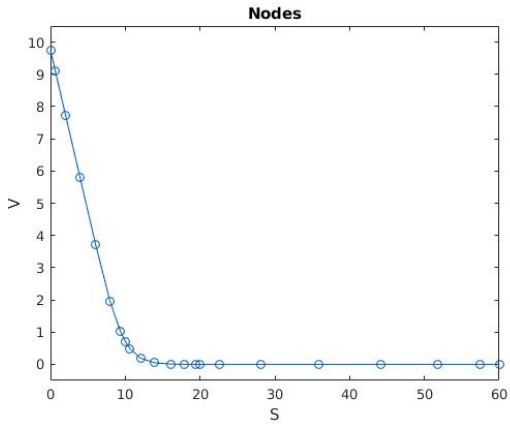

(b) Distribution of option values V corresponding to the nodes in (a).

Figure 5.1: Distribution of nodes for polynomial degree $N_i = 7$, $i = 1, 2, 3$. In (a) the distribution of nodes is shown along the S-axis while (b) shows the location of each computed option value V based on these nodes.

Numerical solutions obtained by the Legendre Galerkin scheme with domain decomposition for different values of N, are shown in Figure 5.2. Setting $N = 9$ gives the results in Figures 5.2a and 5.2b. The option price for the whole domain $\Omega = (0, S_{\text{max}})$ is shown to the left and the right hand side shows an enlarged image of the option price around the strike price K. The numerical solution exhibits oscillatory behaviour and deviates significantly from the exact solution. Increasing N slightly to $N = 12$ gives the results shown in Figures 5.2c and 5.2d. For this value of N, the oscillatory behaviour is no longer visible. Results for $N = 15$, found in Figures 5.2e and 5.2f, shows a solution very similar to the exact solution.

In order to study the approximation error, we use the norm defined in (5.12) to measure the difference between the approximate solution and the exact solution. The option price V in $S = K$ and the errors related to increasing values of N are shown in Table 5.2.

N	$V(K)$	$\|V_{\text{exact}} - V^N\|_{\tilde{L}^2}$
6	0.832015197804	8.536e-02
12	0.758698688394	2.340e-02
24	0.717556757862	3.485e-04
48	0.716586595173	6.179e-07
72	0.716586784937	1.583e-09
96	0.716586783133	1.909e-12
192	0.716586783128	2.131e-14

Table 5.2: The option price V in $S = K$ and the error measured with the approximated L^2-norm for different values of N.

Convergence of the method with and without domain decomposition is shown in Figure 5.3. When domain decomposition is used we can observe spectral convergence and the error reduces rapidly until it becomes of magnitude 10^{-14}. When domain decomposition is not used and the number of nodes is not refined around K, only second order convergence is achieved. It is interesting to observe that the implementation of domain decomposition restores spectral convergence.

The error associated with the different values of N used in the convergence test is shown in Figure 5.4. The plots show that the dominating error is located near the slope discontinuity of the payoff function in K and at the boundary in $S = 0$.

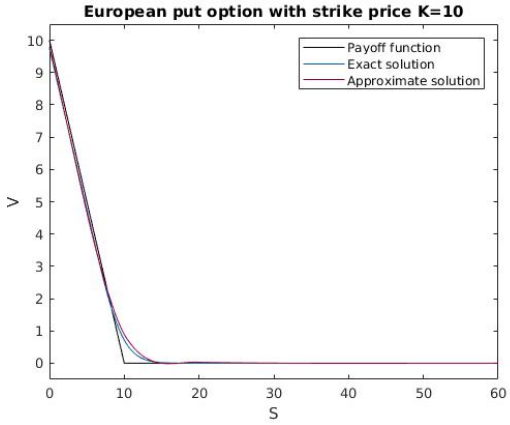

(a) Option price solution obtained with $N = 9$.

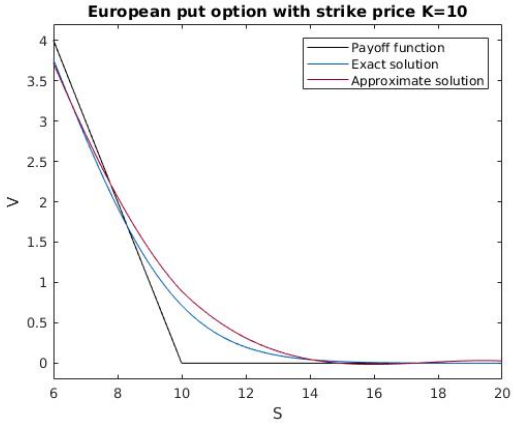

(b) An enlarged image of the case in (a) around the region of rapid change.

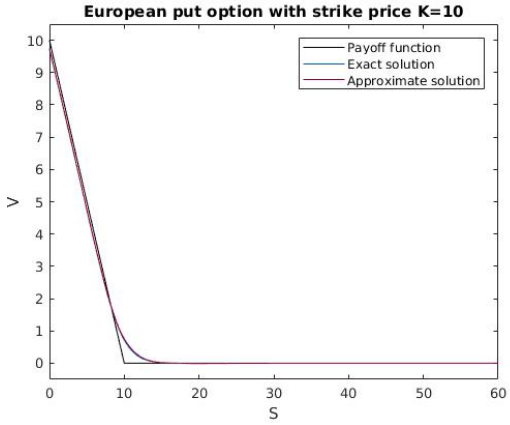

(c) Option price solution obtained with $N = 12$.

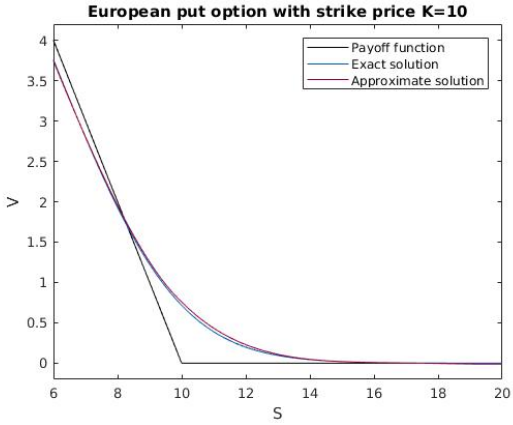

(d) An enlarged image of the case in (c) around the region of rapid change.

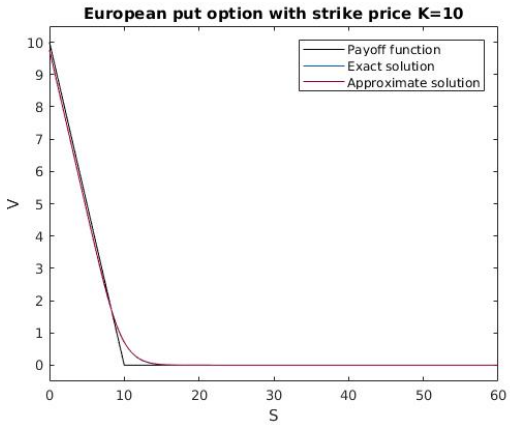

(e) Option price solution obtained with $N = 15$.

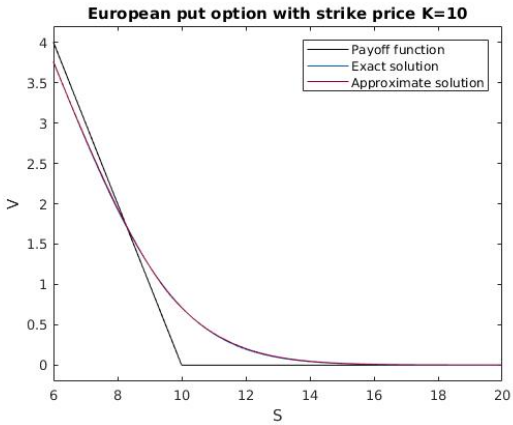

(f) An enlarged image of the case in (e) around the region of rapid change.

Figure 5.2: The solution of the European pricing problem for different values of N compared to the exact solution.

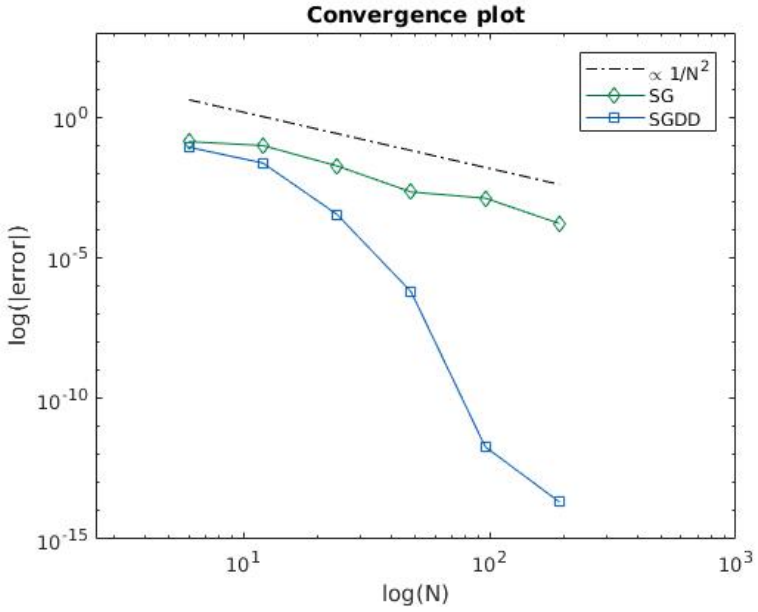

Figure 5.3: Log-log plot showing the convergence of the method with and without domain decomposition for N varying from 6 to 192. SG refers to Spectral Galerkin and SGDD refers to Spectral Galerkin with domain decomposition.

The numerical results indicate that the Legendre Galerkin method with numerical integration and domain decomposition yields spectral convergence for the European pricing problem. The fact that we can obtain a very accurate solution with small N saves memory and computational time and makes the method very competitive to other numerical methods. These results are promising for spectral approximation of more complex option problems that do not admit an available analytical solution.

Remark 2 *As the polynomial order determines the convergence rate, it would be more precise to plot the error in the domain decomposition method against the smallest N_i (simply N_i for equal N_i's) instead of N in the convergence plot. However, the chosen representation makes it easier to compare the two methods for the same number of nodes on the full domain. In following sections, convergence plots will be shown with error plotted against N_i.*

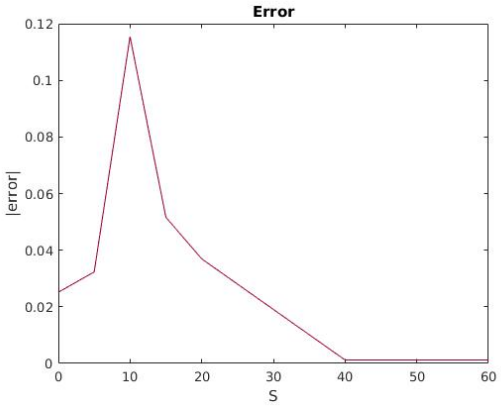

(a) Error between the numerical solution and the exact solution for $N = 6$.

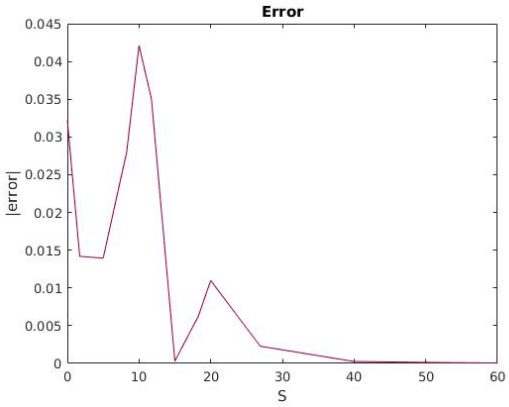

(b) Error between the numerical solution and the exact solution for $N = 12$.

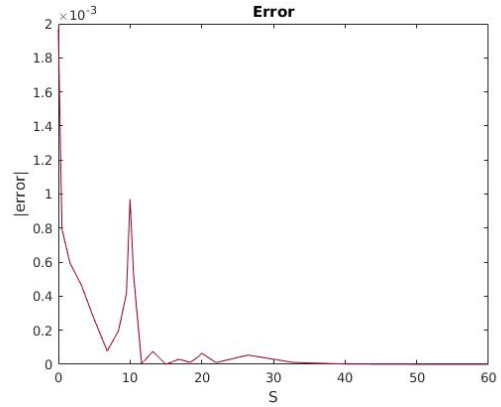

(c) Error between the numerical solution and the exact solution for $N = 24$.

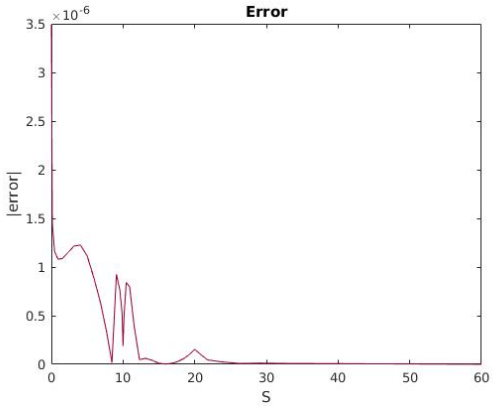

(d) Error between the numerical solution and the exact solution for $N = 48$.

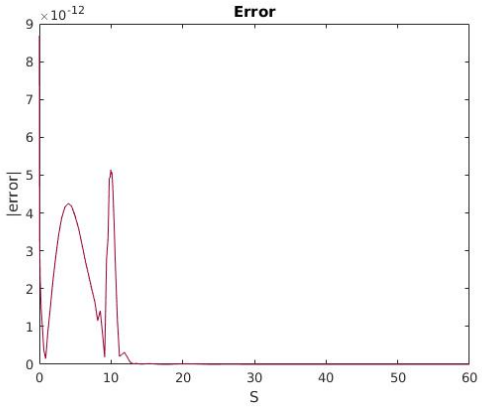

(e) Error between the numerical solution and the exact solution for $N = 96$.

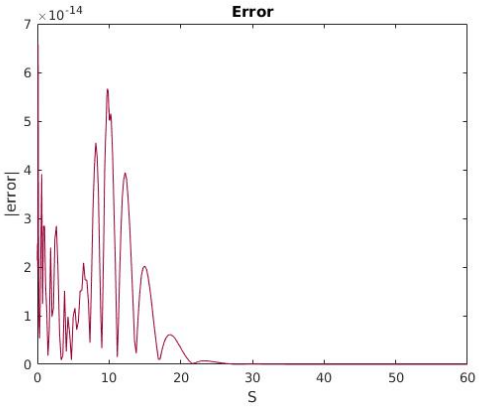

(f) Error between the numerical solution and the exact solution for $N = 192$.

Figure 5.4: Error between the numerical solution and the exact solution for different values of N ranging from $N = 6$ to $N = 192$.

Chapter 6

The Two-Asset European Pricing Problem

6.1 A Legendre Galerkin Scheme with Numerical Integration

Here, we extend the previous work to two dimensions and solve the two-asset Black-Scholes equation (3.15) with payoff function (3.16c). Originally, this problem is defined on the infinite domain $\left\{\mathbf{S} = (S_1, S_2) \in \mathbb{R}^2_+\right\}$. In order to solve the problem numerically, the domain needs to be truncated. For simplicity, we consider a quadratic domain and restrict the domain to $\Omega = [0, S_{\text{max}}]^2$, with S_{max} sufficiently large.

As boundary conditions we take

$$\frac{\partial V}{\partial S_1} = 0 \Big|_{S_1 = S_{\text{max}}} \quad \text{and} \quad \frac{\partial V}{\partial S_2} = 0 \Big|_{S_2 = S_{\text{max}}}. \tag{6.1}$$

It is not necessary to impose boundary conditions on the remaining boundary since the equation itself reduces to a natural boundary condition in $\{S_1 = 0, S_2 \in [0, S_{\text{max}}]\}$ and $\{S_2 = 0, S_1 \in [0, S_{\text{max}}]\}$. After deriving the weak formulation of the problem we will see that the above boundary conditions will be natural boundary conditions for our problem.

Now, we would like to form a two-dimensional expansion based on the Legendre Gauss-Lobatto quadrature formula and one-dimensional basis functions used earlier. A natural way to do this is by tensorization [13].

Let $\{x_j, w_j\}_{j=0,...,N}$ be the $N+1$ nodes and weights of the Legendre Gauss-Lobatto quadrature formula in the closed domain $d = [-1, 1]$. Then, by tensorization, we obtain the $(N+1)^2$ nodes and weights $\{\mathbf{x_k}, w_\mathbf{k}\}_{\mathbf{k}\in K}$ of the corresponding formula in $D = [-1, 1]^2$, with $K = \{\mathbf{k} = (k_1, k_2) \,|\, k_1 = 0, ..., N,\ k_2 = 0, ..., N\}$. This formula satisfies

$$\int_D p(\mathbf{x})d\mathbf{x} \approx \sum_{\mathbf{k}\in K} w_\mathbf{k} p(\mathbf{x_k}), \tag{6.2}$$

and is exact for all polynomials on D of degree less or equal to $2N-1$.

Next, we expand the basis functions used in the one-dimensional case in order to define trial and test function suitable for the two-dimensional case.

Given two families $\{\psi_{k_l}^{(l)}\}_{k_l}$ of one-dimensional basis functions on intervals d, with ψ_{k_l} as defined in (5.1), then the family $\{\psi_\mathbf{k}(\mathbf{x})\}_\mathbf{k}$, defined through

$$\psi_\mathbf{k}(\mathbf{x}) = \psi_{k_1}^{(1)}(x_1)\psi_{k_2}^{(2)}(x_2), \quad \mathbf{k} = (k_1, k_2),\ \mathbf{x} = (x_1, x_2), \tag{6.3}$$

is a two-dimensional basis on the domain D. Now $\psi_\mathbf{k}$ defines a characteristic Lagrange polynomial relative to the N-degree tensorized Legendre-Gauss-Lobatto points in D (see [13], Section 2.8). The functions in (6.3) will be our trial and test functions. An approximate solution is then sought in the form

$$V^N(\mathbf{x}, t) = \sum_{\mathbf{n}\in K} V_\mathbf{n}(t)\psi_\mathbf{n}(\mathbf{x}). \tag{6.4}$$

Now, we derive the weak formulation of the problem (3.15), on the truncated domain Ω. Multiplying the equation with any of the test functions and integrating over the domain gives

$$\begin{aligned}&\int_\Omega \frac{\partial V}{\partial t}\psi_\mathbf{k} d\mathbf{S} + \frac{1}{2}\sigma_1^2 \int_\Omega S_1^2 \frac{\partial^2 V}{\partial S_1^2}\psi_\mathbf{k} d\mathbf{S} + \frac{1}{2}\sigma_2^2 \int_\Omega S_2^2 \frac{\partial^2 V}{\partial S_2^2}\psi_\mathbf{k} d\mathbf{S} + r\int_\Omega S_1 \frac{\partial V}{\partial S_1}\psi_\mathbf{k} d\mathbf{S} \\ &+ r\int_\Omega S_2 \frac{\partial V}{\partial S_2}\psi_\mathbf{k} d\mathbf{S} - r\int_\Omega V\psi_\mathbf{k} d\mathbf{S} \;=\; 0, \qquad \mathbf{k} \in K.\end{aligned}$$

Let $\partial\Omega = \Gamma_1 \cup \Gamma_2 \cup \Gamma_3 \cup \Gamma_4$ where $\Gamma_1 = \{S_2 = 0, S_1 \in [0, S_{\text{max}}]\}$, $\Gamma_2 = \{S_1 = S_{\text{max}}, S_2 \in [0, S_{\text{max}}]\}$, $\Gamma_3 = \{S_2 = S_{\text{max}}, S_1 \in [0, S_{\text{max}}]\}$ and $\Gamma_4 = \{S_1 = 0, S_2 \in [0, S_{\text{max}}]\}$. Using integration by parts on the two terms with second derivatives and applying the boundary conditions (6.1) yields

$$
\begin{aligned}
&\frac{1}{2}\sigma_1^2\int_\Omega S_1^2\frac{\partial^2 V}{\partial S_1^2}\psi_{\mathbf{k}}d\mathbf{S}+\frac{1}{2}\sigma_2^2\int_\Omega S_2^2\frac{\partial^2 V}{\partial S_2^2}\psi_{\mathbf{k}}d\mathbf{S}\\
&=\frac{1}{2}\sigma_1^2\int_{\Gamma_4} S_1^2\frac{\partial V}{\partial S_1}\psi_{\mathbf{k}}dS_2+\frac{1}{2}\sigma_2^2\int_{\Gamma_1} S_2^2\frac{\partial V}{\partial S_2}\psi_{\mathbf{k}}dS_1+\frac{1}{2}\sigma_1^2\int_{\Gamma_3} S_1^2\frac{\partial V}{\partial S_1}\psi_{\mathbf{k}}dS_1\\
&+\frac{1}{2}\sigma_1^2\int_{\Gamma_2} S_2^2\frac{\partial V}{\partial S_2}\psi_{\mathbf{k}}dS_2-\sigma_1^2\int_\Omega S_1\frac{\partial V}{\partial S_1}\psi_{\mathbf{k}}d\mathbf{S}-\frac{1}{2}\sigma_1^2\int_\Omega S_1^2\frac{\partial V}{\partial S_1}\frac{\partial\psi_{\mathbf{k}}}{\partial S_1}d\mathbf{S}\\
&-\sigma_2^2\int_\Omega S_2\frac{\partial V}{\partial S_2}\psi_{\mathbf{k}}d\mathbf{S}-\frac{1}{2}\sigma_2^2\int_\Omega S_2^2\frac{\partial V}{\partial S_2}\frac{\partial\psi_{\mathbf{k}}}{\partial S_2}d\mathbf{S}\\
&=-\sigma_1^2\int_\Omega S_1\frac{\partial V}{\partial S_1}\psi_{\mathbf{k}}d\mathbf{S}-\frac{1}{2}\sigma_1^2\int_\Omega S_1^2\frac{\partial V}{\partial S_1}\frac{\partial\psi_{\mathbf{k}}}{\partial S_1}d\mathbf{S}-\sigma_2^2\int_\Omega S_2\frac{\partial V}{\partial S_2}\psi_{\mathbf{k}}d\mathbf{S}\\
&-\frac{1}{2}\sigma_2^2\int_\Omega S_2^2\frac{\partial V}{\partial S_2}\frac{\partial\psi_{\mathbf{k}}}{\partial S_2}d\mathbf{S},
\end{aligned}
$$

after noticing that $S_1=0$ on Γ_4 and $S_2=0$ on Γ_1.

This gives the integral conditions

$$
\begin{aligned}
&\int_\Omega\frac{\partial V}{\partial t}\psi_{\mathbf{k}}d\mathbf{S}-(\sigma_1^2-r)\int_\Omega S_1\frac{\partial V}{\partial S_1}\psi_{\mathbf{k}}d\mathbf{S}-\frac{1}{2}\sigma_1^2\int_\Omega S_1^2\frac{\partial V}{\partial S_1}\frac{\partial\psi_{\mathbf{k}}}{\partial S_1}d\mathbf{S}\\
&-(\sigma_2^2-r)\int_\Omega S_2\frac{\partial V}{\partial S_2}\psi_{\mathbf{k}}d\mathbf{S}-\frac{1}{2}\sigma_2^2\int_\Omega S_2^2\frac{\partial V}{\partial S_2}\frac{\partial\psi_{\mathbf{k}}}{\partial S_2}d\mathbf{S}-r\int_\Omega V\psi_{\mathbf{k}}d\mathbf{S}\;=\;0,\qquad \mathbf{k}\in K.
\end{aligned}
\tag{6.5}
$$

Let us now define

$$
\begin{aligned}
(V,\psi)&=\int_\Omega V\psi d\mathbf{S}\\
a(V,\psi)&=-(\sigma_1^2-r)\int_\Omega S_1\frac{\partial V}{\partial S_1}\psi_{\mathbf{k}}d\mathbf{S}-\frac{1}{2}\sigma_1^2\int_\Omega S_1^2\frac{\partial V}{\partial S_1}\frac{\partial\psi_{\mathbf{k}}}{\partial S_1}d\mathbf{S}\\
&\quad-(\sigma_2^2-r)\int_\Omega S_2\frac{\partial V}{\partial S_2}\psi_{\mathbf{k}}d\mathbf{S}-\frac{1}{2}\sigma_2^2\int_\Omega S_2^2\frac{\partial V}{\partial S_2}\frac{\partial\psi_{\mathbf{k}}}{\partial S_2}d\mathbf{S}-r\int_\Omega V\psi_{\mathbf{k}}d\mathbf{S},
\end{aligned}
$$

then the weak formulation becomes

$$
\begin{cases}
\text{For } t\in(0,T) \text{ a.e., find } V(t) \text{ such that}\\
\frac{d}{dt}(V(t),\psi_{\mathbf{k}})+a(V(t),\psi_{\mathbf{k}})=0,\quad \mathbf{k}\in K\\
V|_{t=T}=V_\circ,
\end{cases}
\tag{6.6}
$$

where $V_\circ$ is the payoff function in (3.16c).

Since the chosen quadrature nodes are distributed over the closure of the interval $\hat{\Omega} = (-1,1)^2$, we perform a transformation to this reference domain. The mapping used for S_1 and S_2 is

$$\begin{aligned} S_1(\xi_1) &= \frac{S_{\max} - S_{\min}}{2}(\xi_1 + 1) + S_{\min}, \qquad & \frac{\partial S_1}{\partial \xi_1} &= \frac{S_{\max} - S_{\min}}{2}, \\ S_2(\xi_2) &= \frac{S_{\max} - S_{\min}}{2}(\xi_2 + 1) + S_{\min}, \qquad & \frac{\partial S_2}{\partial \xi_2} &= \frac{S_{\max} - S_{\min}}{2}. \end{aligned} \tag{6.7}$$

For $S_{\min} = 0$, this becomes

$$\begin{aligned} S_1(\xi_1) &= \frac{S_{\max}}{2}(\xi_1 + 1), \qquad & \frac{\partial S_1}{\partial \xi_1} &= \frac{S_{\max}}{2}, \\ S_2(\xi_2) &= \frac{S_{\max}}{2}(\xi_2 + 1), \qquad & \frac{\partial S_2}{\partial \xi_2} &= \frac{S_{\max}}{2}. \end{aligned}$$

In particular, the Jacobian is given by $J = {}^{S^2_{\max}}/_4$.

With this choice of mapping the weak formulation (6.5) can be written as

$$\begin{aligned} &J \int_{\hat{\Omega}} \frac{\partial V}{\partial t}\psi_{\mathbf{k}} d\boldsymbol{\xi} - \frac{1}{2} S_{\max}(\sigma_1^2 - r) \int_{\hat{\Omega}} S_1(\xi_1) \frac{\partial V}{\partial \xi_1}\psi_{\mathbf{k}} d\boldsymbol{\xi} - \frac{1}{2}\sigma_1^2 \int_{\hat{\Omega}} S_1^2(\xi_1) \frac{\partial V}{\partial \xi_1}\frac{\partial \psi_{\mathbf{k}}}{\partial \xi_1} d\boldsymbol{\xi} \\ &- \frac{1}{2} S_{\max}(\sigma_2^2 - r) \int_{\hat{\Omega}} S_2(\xi_2) \frac{\partial V}{\partial \xi_2}\psi_{\mathbf{k}} d\boldsymbol{\xi} - \frac{1}{2}\sigma_2^2 \int_{\hat{\Omega}} S_2^2(\xi_2) \frac{\partial V}{\partial \xi_2}\frac{\partial \psi_{\mathbf{k}}}{\partial \xi_2} d\boldsymbol{\xi} - rJ \int_{\hat{\Omega}} V \psi_{\mathbf{k}} d\boldsymbol{\xi} \;=\; 0, \quad \mathbf{k} \in K. \end{aligned}$$

These are the equations we also ask the approximate solution V^N to satisfy. Replacing V with V^N yields the numerical scheme

$$\begin{aligned} &J \int_{\hat{\Omega}} \frac{\partial V^N}{\partial t}\psi_{\mathbf{k}} d\boldsymbol{\xi} - \frac{1}{2} S_{\max}(\sigma_1^2 - r) \int_{\hat{\Omega}} S_1(\xi_1) \frac{\partial V^N}{\partial \xi_1}\psi_{\mathbf{k}} d\boldsymbol{\xi} \\ &- \frac{1}{2}\sigma_1^2 \int_{\hat{\Omega}} S_1^2(\xi_1) \frac{\partial V^N}{\partial \xi_1}\frac{\partial \psi_{\mathbf{k}}}{\partial \xi_1} d\boldsymbol{\xi} - \frac{1}{2} S_{\max}(\sigma_2^2 - r) \int_{\hat{\Omega}} S_2(\xi_2) \frac{\partial V^N}{\partial \xi_2}\psi_{\mathbf{k}} d\boldsymbol{\xi} \\ &- \frac{1}{2}\sigma_2^2 \int_{\hat{\Omega}} S_2^2(\xi_2) \frac{\partial V^N}{\partial \xi_2}\frac{\partial \psi_{\mathbf{k}}}{\partial \xi_2} d\boldsymbol{\xi} - rJ \int_{\hat{\Omega}} V^N \psi_{\mathbf{k}} d\boldsymbol{\xi} \;=\; 0, \qquad \mathbf{k} \in K. \end{aligned} \tag{6.8}$$

We again resort to numerical integration in order to evaluate the above integrals and choose the Gauss-Lobatto quadrature formula (6.2). Applying it to the integrals in equation (6.8) gives the scheme

$$
\begin{aligned}
&J\sum_{\mathbf{l}\in K} w_{\mathbf{l}}\left(\frac{\partial V^N}{\partial t}\psi_{\mathbf{k}}\right)(\boldsymbol{\xi}_{\mathbf{l}}) - \frac{S_{\max}}{2}(\sigma_1^2 - r)\sum_{\mathbf{l}\in K} w_{\mathbf{l}}\left(S_1\frac{\partial V^N}{\partial \xi_1}\psi_{\mathbf{k}}\right)(\boldsymbol{\xi}_{\mathbf{l}}) \\
&-\frac{\sigma_1^2}{2}\sum_{\mathbf{l}\in K} w_{\mathbf{l}}\left(S_1^2\frac{\partial V^N}{\partial \xi_1}\frac{\partial \psi_{\mathbf{k}}}{\partial \xi_1}\right)(\boldsymbol{\xi}_{\mathbf{l}}) - \frac{S_{\max}}{2}(\sigma_2^2 - r)\sum_{\mathbf{l}\in K} w_{\mathbf{l}}\left(S_2\frac{\partial V^N}{\partial \xi_2}\psi_{\mathbf{k}}\right)(\boldsymbol{\xi}_{\mathbf{l}}) \qquad (6.9)\\
&-\frac{\sigma_2^2}{2}\sum_{\mathbf{l}\in K} w_{\mathbf{l}}\left(S_2^2\frac{\partial V^N}{\partial \xi_2}\frac{\partial \psi_{\mathbf{k}}}{\partial \xi_2}\right)(\boldsymbol{\xi}_{\mathbf{l}}) - rJ\sum_{\mathbf{l}\in K} w_{\mathbf{l}}\left(V^N\psi_{\mathbf{k}}\right)(\boldsymbol{\xi}_{\mathbf{l}}) \;=\; 0, \qquad \mathbf{k}\in K.
\end{aligned}
$$

As in the one-dimensional case we can observe that the terms inside the sums are polynomials of degree $2N$, hence our quadrature formula is not exact. However, we proceed with this approach, despite introducing a small error.

6.2 The Scheme as a System of Algebraic Equations

The scheme (6.9) can be reformulated as a system $M\dot{V} + AV = 0$ of algebraic equations by inserting the expansion (6.4) for V^N. This gives the following system

$$
\sum_{\mathbf{n}\in K} M_{\mathbf{kn}}\frac{dV_{\mathbf{n}}}{dt} + \sum_{\mathbf{n}\in K} A_{\mathbf{kn}}V_{\mathbf{n}} = 0, \qquad \mathbf{k}\in K,
$$

where $V_{\mathbf{n}}$ are the unknowns and the matrix entries are given by

$$
M_{\mathbf{kn}} = J\sum_{\mathbf{l}\in K} w_{\mathbf{l}}\psi_{\mathbf{n}}(\boldsymbol{\xi}_{\mathbf{l}})\psi_{\mathbf{k}}(\boldsymbol{\xi}_{\mathbf{l}})
$$

and

$$
\begin{aligned}
A_{\mathbf{kn}} = &-\frac{\sigma_1^2}{2}\sum_{\mathbf{l}\in K} w_{\mathbf{l}}\left(S_1^2\frac{d\psi_{\mathbf{n}}}{d\xi_1}\frac{d\psi_{\mathbf{k}}}{d\xi_1}\right)(\boldsymbol{\xi}_{\mathbf{l}}) - \frac{S_{\max}}{2}(\sigma_1^2 - r)\sum_{\mathbf{l}\in K} w_{\mathbf{l}}\left(S_1\frac{d\psi_{\mathbf{n}}}{d\xi_1}\psi_{\mathbf{k}}\right)(\boldsymbol{\xi}_{\mathbf{l}}) \\
&-\frac{\sigma_2^2}{2}\sum_{\mathbf{l}\in K} w_{\mathbf{l}}\left(S_2^2\frac{d\psi_{\mathbf{n}}}{d\xi_2}\frac{d\psi_{\mathbf{k}}}{d\xi_2}\right)(\boldsymbol{\xi}_{\mathbf{l}}) - \frac{S_{\max}}{2}(\sigma_2^2 - r)\sum_{\mathbf{l}\in K} w_{\mathbf{l}}\left(S_2\frac{d\psi_{\mathbf{n}}}{d\xi_2}\psi_{\mathbf{k}}\right)(\boldsymbol{\xi}_{\mathbf{l}}) \\
&- rJ\sum_{\mathbf{l}\in K} w_{\mathbf{l}}\left(\psi_{\mathbf{n}}\psi_{\mathbf{k}}\right)(\boldsymbol{\xi}_{\mathbf{l}}).
\end{aligned}
$$

Using the properties of the Lagrange polynomials $\psi_{\mathbf{k}}$ and $\psi_{\mathbf{n}}$, the expressions for $M_{\mathbf{kn}}$ and $A_{\mathbf{kn}}$ can be simplified to

$$M_{\mathbf{kn}} = Jw_{\mathbf{k}}\delta_{\mathbf{kn}},$$

and

$$\begin{aligned} A_{\mathbf{kn}} = &- \frac{\sigma_1^2}{2}\sum_{\mathbf{l}\in K} w_{\mathbf{l}} \left(S_1^2 \frac{d\psi_{\mathbf{n}}}{d\xi_1}\frac{d\psi_{\mathbf{k}}}{d\xi_1} \right)(\boldsymbol{\xi}_{\mathbf{l}}) - \frac{S_{\max}}{2}(\sigma_1^2 - r) w_{\mathbf{k}} \left(S_1 \frac{d\psi_{\mathbf{n}}}{d\xi_1} \right)(\boldsymbol{\xi}_{\mathbf{k}}) \\ &- \frac{\sigma_2^2}{2}\sum_{\mathbf{l}\in K} w_{\mathbf{l}} \left(S_2^2 \frac{d\psi_{\mathbf{n}}}{d\xi_2}\frac{d\psi_{\mathbf{k}}}{d\xi_2} \right)(\boldsymbol{\xi}_{\mathbf{l}}) - \frac{S_{\max}}{2}(\sigma_2^2 - r) w_{\mathbf{k}} \left(S_2 \frac{d\psi_{\mathbf{n}}}{d\xi_2} \right)(\boldsymbol{\xi}_{\mathbf{k}}) \\ &- rJw_{\mathbf{k}}\delta_{\mathbf{kn}}. \end{aligned}$$

A numerical solution can now be obtained by solving the linear system $M\dot{V}(t) + AV(t) = 0$ using an appropriate solver for ordinary differential equations, such as the time-stepping method in (5.11).

In order to evaluate the accuracy of the numerical scheme, we generalize the approximated L^2-norm given in (5.12):

$$\begin{aligned} \|V_{\text{exact}}(\cdot,t) - V^N(\cdot,t)\| &= \left(\int_{\hat{\Omega}} |V_{\text{exact}}(\boldsymbol{\xi},t) - V^N(\boldsymbol{\xi},t)|^2 d\boldsymbol{\xi} \right)^{1/2} \\ &\approx \left(\sum_{\mathbf{k}\in K} w_{\mathbf{k}} |V_{\text{exact}}(\boldsymbol{\xi}_{\mathbf{k}},t) - V^N(\boldsymbol{\xi}_{\mathbf{k}},t)|^2 \right)^{1/2} = \|V_{\text{exact}}(\cdot,t) - V^N(\cdot,t)\|_{\tilde{L}^2}, \end{aligned} \tag{6.10}$$

with t being some fixed time, and $w_{\mathbf{k}}$ and $\boldsymbol{\xi}_{\mathbf{k}}$ being the tensorized Legendre Gauss-Lobatto weights and nodes, respectively.

6.3 A Numerical Scheme with Domain Decomposition

In the following we develop a numerical scheme with domain decomposition for the two-asset problem (6.6). We choose to divide the domain Ω into four subdomains:

$$\begin{aligned} \Omega_1 &= \left\{ \mathbf{S} = (S_1, S_2) \in \mathbb{R}^2_+ \mid S_1 \le K, S_2 \le K \right\}, \\ \Omega_2 &= \left\{ \mathbf{S} = (S_1, S_2) \in \mathbb{R}^2_+ \mid K \le S_1 \le S_{\max}, S_2 \le K \right\}, \\ \Omega_3 &= \left\{ \mathbf{S} = (S_1, S_2) \in \mathbb{R}^2_+ \mid K \le S_1 \le S_{\max}, K \le S_2 \le S_{\max} \right\}, \\ \Omega_4 &= \left\{ \mathbf{S} = (S_1, S_2) \in \mathbb{R}^2_+ \mid S_1 \le K, K \le S_2 \le S_{\max} \right\}. \end{aligned}$$

Let the interface of the subdomains be specified as follows

$$\gamma_1 := \{S_1 = K, S_2 \in [0, K]\},$$

$$\gamma_2 := \{S_1 \in [K, S_{\max}], S_2 = K\},$$

$$\gamma_3 := \{S_1 = K, S_2 \in [K, S_{\max}]\},$$

$$\gamma_4 := \{S_1 \in [0, K], S_2 = K\}.$$

The partition of Ω in the case where $K = 100$ and $S_{\max} = 200$ is shown in Figure 6.1.

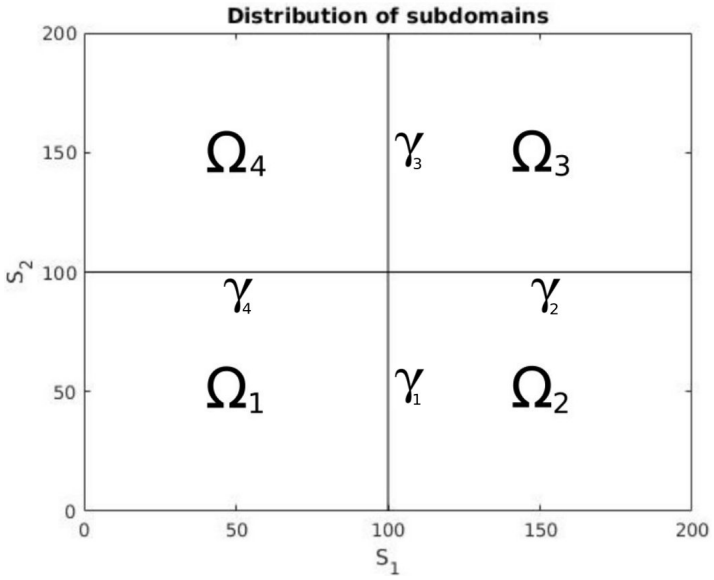

Figure 6.1: Distribution of subdomains, Ω_i for $i = 1, 2, 3, 4$, in the domain decomposition method when $K = 100$ and $S_{\max} = 200$.

Let us indicate by $V^{(i)}$ the restriction of the solution V of (6.6) to Ω_i, $i = 1, 2, 3, 4$ and define

$$\begin{aligned}
\left(V^{(i)}, \psi^{(i)}\right)_{\Omega_i} &= \int_{\Omega_i} V^{(i)}\psi^{(i)} d\mathbf{S} \\
a_i\left(V^{(i)}, \psi^{(i)}\right) &= \frac{1}{2}\sigma_1^2 \int_{\gamma^{(i,1)}} K^2 \frac{\partial V^{(i)}}{\partial S_1}\psi^{(i)} dS_2 + \frac{1}{2}\sigma_2^2 \int_{\gamma^{(i,2)}} K^2 \frac{\partial V^{(i)}}{\partial S_2}\psi^{(i)} dS_1 \\
&\quad - (\sigma_1^2 - r)\int_{\Omega_i} S_1 \frac{\partial V^{(i)}}{\partial S_1}\psi^{(i)} d\mathbf{S} - \frac{1}{2}\sigma_1^2 \int_{\Omega_i} S_1^2 \frac{\partial V^{(i)}}{\partial S_1}\frac{\partial \psi^{(i)}}{\partial S_1} d\mathbf{S} \\
&\quad - (\sigma_2^2 - r)\int_{\Omega_i} S_2 \frac{\partial V^{(i)}}{\partial S_2}\psi^{(i)} d\mathbf{S} - \frac{1}{2}\sigma_2^2 \int_{\Omega_i} S_2^2 \frac{\partial V^{(i)}}{\partial S_2}\frac{\partial \psi^{(i)}}{\partial S_2} d\mathbf{S} \\
&\quad - r\int_{\Omega_i} V^{(i)}\psi^{(i)} d\mathbf{S},
\end{aligned} \tag{6.11}$$

where $\psi^{(i)}$ are the test functions associated with the nodes lying in the closed subdomain $\overline{\Omega}_i$ and $\gamma^{(i,1)}, \gamma^{(i,2)}$ are given by

$$\begin{aligned}
&\gamma^{(1,1)} = \gamma_1, \quad \gamma^{(1,2)} = \gamma_4 \\
&\gamma^{(2,1)} = \gamma_1, \quad \gamma^{(2,2)} = \gamma_2 \\
&\gamma^{(3,1)} = \gamma_3, \quad \gamma^{(3,2)} = \gamma_2 \\
&\gamma^{(4,1)} = \gamma_3, \quad \gamma^{(4,2)} = \gamma_4.
\end{aligned}$$

On each subdomain we choose again the N_i-th degree polynomials defined in (5.1) as test function. Furthermore, let us denote by K_i the set of nodes lying in the closed subdomain $\overline{\Omega}_i$, i.e. $K_i = \{\mathbf{k} = (k_1, k_2) \,|\, k_1 = 0, ..., N_i,\ k_2 = 0, ..., N_i\}$, $i = 1, 2, 3, 4$. Then the problem in (6.6) admits the following equivalent four-domain formulation, for $t \in (0, T)$ a.e.:

$$\begin{cases} \frac{d}{dt}\left(u^{(i)}(t), \psi_{\mathbf{k}}^{(i)}\right)_{\Omega_i} + a_i\left(u^{(i)}(t), \psi_{\mathbf{k}}^{(i)}\right) = 0 \\ V^{(i)}(0) = V_{\circ|\Omega_i}, \qquad \mathbf{k} = 0, ..., K_i, \quad i = 1, 2, 3, 4, \end{cases} \tag{6.12}$$

where in addition the following interface conditions are to be satisfied

$$\begin{cases} V^{(1)}(\mathbf{S}) = V^{(2)}(\mathbf{S}) \\ \frac{\partial V^{(1)}}{\partial n}(\mathbf{S}) = -\frac{\partial V^{(2)}}{\partial n}(\mathbf{S}), \qquad \mathbf{S} \in \partial\Omega_1 \cap \partial\Omega_2 \\ V^{(2)}(\mathbf{S}) = V^{(3)}(\mathbf{S}) \\ \frac{\partial V^{(2)}}{\partial n}(\mathbf{S}) = -\frac{\partial V^{(3)}}{\partial n}(\mathbf{S}), \qquad \mathbf{S} \in \partial\Omega_2 \cap \partial\Omega_3 \\ V^{(3)}(\mathbf{S}) = V^{(4)}(\mathbf{S}) \\ \frac{\partial V^{(3)}}{\partial n}(\mathbf{S}) = -\frac{\partial V^{(4)}}{\partial n}(\mathbf{S}), \qquad \mathbf{S} \in \partial\Omega_3 \cap \partial\Omega_4 \\ V^{(1)}(\mathbf{S}) = V^{(4)}(\mathbf{S}) \\ \frac{\partial V^{(1)}}{\partial n}(\mathbf{S}) = -\frac{\partial V^{(4)}}{\partial n}(\mathbf{S}), \qquad \mathbf{S} \in \partial\Omega_1 \cap \partial\Omega_4. \end{cases} \tag{6.13}$$

We now map each subdomain to the reference domain $\hat{\Omega} = (-1, 1)^2$ through the linear transformation

$$\begin{cases} S_1(\xi_1) = \frac{K}{2}(\xi_1+1), \quad S_2(\xi_2) = \frac{K}{2}(\xi_2+1), & \mathbf{S} \in \Omega_1 \\ S_1(\xi_1) = \frac{S_{\max}-K}{2}(\xi_1+1)+K, \quad S_2(\xi_2) = \frac{K}{2}(\xi_2+1), & \mathbf{S} \in \Omega_2 \\ S_1(\xi_1) = \frac{S_{\max}-K}{2}(\xi_1+1)+K, \quad S_2(\xi_2) = \frac{S_{\max}-K}{2}(\xi_2+1)+K, & \mathbf{S} \in \Omega_3, \\ S_1(\xi_1) = \frac{K}{2}(\xi_1+1), \quad S_2(\xi_2) = \frac{S_{\max}-K}{2}(\xi_2+1)+K, & \mathbf{S} \in \Omega_4, \end{cases}$$

calculated from (6.7).

Based on this, we denote

$$\begin{cases} J_1^{(1)} := \frac{\partial S_1}{\partial \xi_1} = \frac{K}{2}, \quad J_1^{(2)} := \frac{\partial S_2}{\partial \xi_2} = \frac{K}{2}, & \mathbf{S} \in \Omega_1 \\ J_2^{(1)} := \frac{\partial S_1}{\partial \xi_1} = \frac{S_{\max}-K}{2}, \quad J_2^{(2)} := \frac{\partial S_2}{\partial \xi_2} = \frac{K}{2}, & \mathbf{S} \in \Omega_2 \\ J_3^{(1)} := \frac{\partial S_1}{\partial \xi_1} = \frac{S_{\max}-K}{2}, \quad J_3^{(2)} := \frac{\partial S_2}{\partial \xi_2} = \frac{S_{\max}-K}{2}, & \mathbf{S} \in \Omega_3, \\ J_4^{(1)} := \frac{\partial S_1}{\partial \xi_1} = \frac{K}{2}, \quad J_4^{(2)} := \frac{\partial S_2}{\partial \xi_2} = \frac{S_{\max}-K}{2}, & \mathbf{S} \in \Omega_4, \end{cases}$$

and in particular the Jacobian of each element is given by

$$J = \begin{cases} \frac{K^2}{4}, & \mathbf{S} \in \Omega_1 \\ \frac{K(S_{\max}-K)}{4}, & \mathbf{S} \in \Omega_2 \\ \frac{(S_{\max}-K)^2}{4}, & \mathbf{S} \in \Omega_3 \\ \frac{K(S_{\max}-K)}{4}, & \mathbf{S} \in \Omega_4. \end{cases}$$

Denoting $J_i = J_{|\Omega_i}$, this gives the new formulation of (6.11)

$$\left(V^{(i)},\psi^{(i)}\right)_{\hat{\Omega}} = J_i \int_{\hat{\Omega}} V^{(i)}\psi^{(i)} d\boldsymbol{\xi}$$

$$\begin{aligned} a_i\left(V^{(i)},\psi^{(i)}\right) = & \frac{1}{2}\frac{J_i^{(2)}}{J_i^{(1)}}\sigma_1^2 \int_{\hat{\gamma}^{(i,1)}} K^2 \frac{\partial V^{(i)}}{\partial \xi_1}\psi^{(i)} d\xi_2 + \frac{1}{2}\frac{J_i^{(1)}}{J_i^{(2)}}\sigma_2^2 \int_{\hat{\gamma}^{(i,2)}} K^2 \frac{\partial V^{(i)}}{\partial \xi_2}\psi^{(i)} d\xi_1 \\ & - \frac{J_i}{J_i^{(1)}}(\sigma_1^2 - r)\int_{\hat{\Omega}} S_1(\xi_1)\frac{\partial V^{(i)}}{\partial \xi_1}\psi^{(i)} d\boldsymbol{\xi} - \frac{1}{2}\frac{J_i}{(J_i^{(1)})^2}\sigma_1^2 \int_{\hat{\Omega}} S_1^2(\xi_1)\frac{\partial V^{(i)}}{\partial \xi_1}\frac{\partial \psi^{(i)}}{\partial \xi_1} d\boldsymbol{\xi} \\ & - (\sigma_2^2 - r)\frac{J_i}{J_i^{(2)}}\int_{\hat{\Omega}} S_2(\xi_2)\frac{\partial V^{(i)}}{\partial \xi_2}\psi^{(i)} d\boldsymbol{\xi} - \frac{1}{2}\frac{J_i}{(J_i^{(2)})^2}\sigma_2^2 \int_{\hat{\Omega}} S_2^2(\xi_2)\frac{\partial V^{(i)}}{\partial \xi_2}\frac{\partial \psi^{(i)}}{\partial \xi_2} d\boldsymbol{\xi} \\ & - J_i r \int_{\hat{\Omega}} V^{(i)}\psi^{(i)} d\boldsymbol{\xi}, \end{aligned}$$

where $\hat{\gamma}^{(i,1)}, \hat{\gamma}^{(i,2)}$ are the line segments on $\hat{\Omega}$ corresponding to $\gamma^{(i,1)}, \gamma^{(i,2)}$ on Ω.

Upon denoting by $V^{N,(i)}$ the restriction of the approximate solution V^N to Ω_i, the approximate solution is sought in the form

$$V^{N,(i)}(\mathbf{x},t) = \sum_{\mathbf{k}\in K_i} V_{\mathbf{k}}^{(i)}(t)\psi_{\mathbf{k}}^{(i)}(\mathbf{x}), \qquad \mathbf{x}\in\Omega_i, \quad i = 1,2,3,4. \tag{6.14}$$

Let us define $K_{\gamma i}$ to be the set of indices associated with the nodes lying on γ_i. Then, enforcing the conditions in (6.12) and (6.13) on the approximate solution V^N and applying the Gauss-Lobatto quadrature formula (6.2) lets us obtain the numerical scheme

$$
\begin{aligned}
&J_1 \sum_{\mathbf{l}\in K_1} w_{\mathbf{l}} \left(\frac{\partial V^{N,(1)}}{\partial t}\psi_{\mathbf{k}}^{(1)}\right)(\boldsymbol{\xi}_{\mathbf{l}}) + \frac{1}{2}\frac{J_1^{(2)}}{J_1^{(1)}}\sigma_1^2 \sum_{l\in K_{\gamma 1}} K^2 \left(\frac{\partial V^{(N,1)}}{\partial \xi_1}\psi_{\mathbf{k}}^{(1)}\right)(\boldsymbol{\xi}_l) \\
&+ \frac{1}{2}\frac{J_1^{(1)}}{J_1^{(2)}}\sigma_2^2 \sum_{l\in K_{\gamma 4}} K^2 \left(\frac{\partial V^{(N,1)}}{\partial \xi_2}\psi_{\mathbf{k}}^{(1)}\right)(\boldsymbol{\xi}_l) - \frac{1}{2}\frac{J_1}{J_1^{(1)}}(\sigma_1^2 - r)\sum_{\mathbf{l}\in K_1} w_{\mathbf{l}} \left(S_1 \frac{\partial V^{N,(1)}}{\partial \xi_1}\psi_{\mathbf{k}}^{(1)}\right)(\boldsymbol{\xi}_{\mathbf{l}}) \\
&- \frac{1}{2}\frac{J_1}{(J_1^{(1)})^2}\sigma_1^2 \sum_{\mathbf{l}\in K_1} w_{\mathbf{l}} \left(S_1^2 \frac{\partial V^{N,(1)}}{\partial \xi_1}\frac{\partial \psi_{\mathbf{k}}^{(1)}}{\partial \xi_1}\right)(\boldsymbol{\xi}_{\mathbf{l}}) - \frac{1}{2}\frac{J_1}{J_1^{(2)}}(\sigma_2^2 - r)\sum_{\mathbf{l}\in K_1} w_{\mathbf{l}} \left(S_2 \frac{\partial V^{N,(1)}}{\partial \xi_2}\psi_{\mathbf{k}}^{(1)}\right)(\boldsymbol{\xi}_{\mathbf{l}}) \\
&- \frac{1}{2}\frac{J_1}{(J_1^{(2)})^2}\sigma_2^2 \sum_{\mathbf{l}\in K_1} w_{\mathbf{l}} \left(S_2^2 \frac{\partial V^{N,(1)}}{\partial \xi_2}\frac{\partial \psi_{\mathbf{k}}^{(1)}}{\partial \xi_2}\right)(\boldsymbol{\xi}_{\mathbf{l}}) - rJ_1 \sum_{\mathbf{l}\in K_1} w_{\mathbf{l}} \left(V^{N,(1)}\psi_{\mathbf{k}}^{(1)}\right)(\boldsymbol{\xi}_{\mathbf{l}}) \;=\; 0, \;\; \mathbf{k}\in K_1,
\end{aligned}
$$

$$
\begin{aligned}
&J_2 \sum_{\mathbf{l}\in K_2} w_{\mathbf{l}} \left(\frac{\partial V^{N,(2)}}{\partial t}\psi_{\mathbf{k}}^{(2)}\right)(\boldsymbol{\xi}_{\mathbf{l}}) + \frac{1}{2}\frac{J_2^{(2)}}{J_2^{(1)}}\sigma_1^2 \sum_{l\in K_{\gamma 1}} K^2 \left(\frac{\partial V^{(N,1)}}{\partial \xi_1}\psi_{\mathbf{k}}^{(2)}\right)(\boldsymbol{\xi}_l) \\
&+ \frac{1}{2}\frac{J_2^{(1)}}{J_2^{(2)}}\sigma_2^2 \sum_{l\in K_{\gamma 2}} K^2 \left(\frac{\partial V^{(N,i)}}{\partial \xi_2}\psi_{\mathbf{k}}^{(2)}\right)(\boldsymbol{\xi}_l) - \frac{1}{2}\frac{J_2}{J_2^{(1)}}(\sigma_1^2 - r)\sum_{\mathbf{l}\in K_2} w_{\mathbf{l}} \left(S_1 \frac{\partial V^{N,(2)}}{\partial \xi_1}\psi_{\mathbf{k}}^{(2)}\right)(\boldsymbol{\xi}_{\mathbf{l}}) \\
&- \frac{1}{2}\frac{J_2}{(J_2^{(1)})^2}\sigma_1^2 \sum_{\mathbf{l}\in K_2} w_{\mathbf{l}} \left(S_1^2 \frac{\partial V^{N,(2)}}{\partial \xi_1}\frac{\partial \psi_{\mathbf{k}}^{(2)}}{\partial \xi_1}\right)(\boldsymbol{\xi}_{\mathbf{l}}) - \frac{1}{2}\frac{J_2}{J_2^{(2)}}(\sigma_2^2 - r)\sum_{\mathbf{l}\in K_2} w_{\mathbf{l}} \left(S_2 \frac{\partial V^{N,(2)}}{\partial \xi_2}\psi_{\mathbf{k}}^{(2)}\right)(\boldsymbol{\xi}_{\mathbf{l}}) \\
&- \frac{1}{2}\frac{J_2}{(J_2^{(2)})^2}\sigma_2^2 \sum_{\mathbf{l}\in K_2} w_{\mathbf{l}} \left(S_2^2 \frac{\partial V^{N,(2)}}{\partial \xi_2}\frac{\partial \psi_{\mathbf{k}}^{(2)}}{\partial \xi_2}\right)(\boldsymbol{\xi}_{\mathbf{l}}) - rJ_2 \sum_{\mathbf{l}\in K_2} w_{\mathbf{l}} \left(V^{N,(2)}\psi_{\mathbf{k}}^{(2)}\right)(\boldsymbol{\xi}_{\mathbf{l}}) \;=\; 0, \;\; \mathbf{k}\in K_2,
\end{aligned}
$$

$$
\begin{aligned}
&J_3 \sum_{\mathbf{l}\in K_3} w_{\mathbf{l}} \left(\frac{\partial V^{N,(3)}}{\partial t}\psi_{\mathbf{k}}^{(3)}\right)(\boldsymbol{\xi}_{\mathbf{l}}) + \frac{1}{2}\frac{J_3^{(2)}}{J_3^{(1)}}\sigma_1^2 \sum_{l\in K_{\gamma 3}} K^2 \left(\frac{\partial V^{(N,1)}}{\partial \xi_1}\psi_{\mathbf{k}}^{(3)}\right)(\boldsymbol{\xi}_l) \\
&+ \frac{1}{2}\frac{J_3^{(1)}}{J_3^{(2)}}\sigma_2^2 \sum_{l\in K_{\gamma 2}} K^2 \left(\frac{\partial V^{(N,i)}}{\partial \xi_2}\psi_{\mathbf{k}}^{(3)}\right)(\boldsymbol{\xi}_l) - \frac{1}{2}\frac{J_3}{J_3^{(1)}}(\sigma_1^2 - r)\sum_{\mathbf{l}\in K_3} w_{\mathbf{l}} \left(S_1 \frac{\partial V^{N,(3)}}{\partial \xi_1}\psi_{\mathbf{k}}^{(3)}\right)(\boldsymbol{\xi}_{\mathbf{l}}) \\
&- \frac{1}{2}\frac{J_3}{(J_3^{(1)})^2}\sigma_1^2 \sum_{\mathbf{l}\in K_3} w_{\mathbf{l}} \left(S_1^2 \frac{\partial V^{N,(3)}}{\partial \xi_1}\frac{\partial \psi_{\mathbf{k}}^{(3)}}{\partial \xi_1}\right)(\boldsymbol{\xi}_{\mathbf{l}}) - \frac{1}{2}\frac{J_3}{J_3^{(2)}}(\sigma_2^2 - r)\sum_{\mathbf{l}\in K_3} w_{\mathbf{l}} \left(S_2 \frac{\partial V^{N,(3)}}{\partial \xi_2}\psi_{\mathbf{k}}^{(3)}\right)(\boldsymbol{\xi}_{\mathbf{l}}) \\
&- \frac{1}{2}\frac{J_3}{(J_3^{(2)})^2}\sigma_2^2 \sum_{\mathbf{l}\in K_3} w_{\mathbf{l}} \left(S_2^2 \frac{\partial V^{N,(3)}}{\partial \xi_2}\frac{\partial \psi_{\mathbf{k}}^{(3)}}{\partial \xi_2}\right)(\boldsymbol{\xi}_{\mathbf{l}}) - rJ_3 \sum_{\mathbf{l}\in K_3} w_{\mathbf{l}} \left(V^{N,(3)}\psi_{\mathbf{k}}^{(3)}\right)(\boldsymbol{\xi}_{\mathbf{l}}) \;=\; 0, \;\; \mathbf{k}\in K_3,
\end{aligned}
$$

$$
\begin{aligned}
&J_4 \sum_{\mathbf{l}\in K_4} w_{\mathbf{l}} \left(\frac{\partial V^{N,(4)}}{\partial t}\psi_{\mathbf{k}}^{(4)}\right)(\boldsymbol{\xi}_{\mathbf{l}}) + \frac{1}{2}\frac{J_4^{(2)}}{J_4^{(1)}}\sigma_1^2 \sum_{l\in K_{\gamma 3}} K^2 \left(\frac{\partial V^{(N,1)}}{\partial \xi_1}\psi_{\mathbf{k}}^{(4)}\right)(\boldsymbol{\xi}_l) \\
&+ \frac{1}{2}\frac{J_4^{(1)}}{J_4^{(2)}}\sigma_2^2 \sum_{l\in K_{\gamma 4}} K^2 \left(\frac{\partial V^{(N,i)}}{\partial \xi_2}\psi_{\mathbf{k}}^{(4)}\right)(\boldsymbol{\xi}_l) - \frac{1}{2}\frac{J_4}{J_4^{(1)}}(\sigma_1^2 - r)\sum_{\mathbf{l}\in K_4} w_{\mathbf{l}} \left(S_1 \frac{\partial V^{N,(4)}}{\partial \xi_1}\psi_{\mathbf{k}}^{(4)}\right)(\boldsymbol{\xi}_{\mathbf{l}}) \\
&- \frac{1}{2}\frac{J_4}{(J_4^{(1)})^2}\sigma_1^2 \sum_{\mathbf{l}\in K_4} w_{\mathbf{l}} \left(S_1^2 \frac{\partial V^{N,(4)}}{\partial \xi_1}\frac{\partial \psi_{\mathbf{k}}^{(4)}}{\partial \xi_1}\right)(\boldsymbol{\xi}_{\mathbf{l}}) - \frac{1}{2}\frac{J_4}{J_4^{(2)}}(\sigma_2^2 - r)\sum_{\mathbf{l}\in K_4} w_{\mathbf{l}} \left(S_2 \frac{\partial V^{N,(4)}}{\partial \xi_2}\psi_{\mathbf{k}}^{(4)}\right)(\boldsymbol{\xi}_{\mathbf{l}}) \\
&- \frac{1}{2}\frac{J_4}{(J_4^{(2)})^2}\sigma_2^2 \sum_{\mathbf{l}\in K_4} w_{\mathbf{l}} \left(S_2^2 \frac{\partial V^{N,(4)}}{\partial \xi_2}\frac{\partial \psi_{\mathbf{k}}^{(4)}}{\partial \xi_2}\right)(\boldsymbol{\xi}_{\mathbf{l}}) - rJ_4 \sum_{\mathbf{l}\in K_4} w_{\mathbf{l}} \left(V^{N,(4)}\psi_{\mathbf{k}}^{(4)}\right)(\boldsymbol{\xi}_{\mathbf{l}}) \;=\; 0, \;\; \mathbf{k}\in K_4,
\end{aligned}
$$

where the boundary conditions (6.1) have been incorporated in a weak manner and $\boldsymbol{\xi}_{\mathbf{l}}$ and $w_{\mathbf{l}}$ are the tensorized Legendre Gauss-Lobatto nodes and weights, respectively.

After inserting the expansions (6.14) for V^N and incorporating the interface conditions in (6.13), we can rephrase this scheme as a system $M\dot{V} + AV = 0$ of algebraic equations which can be written in the form (5.15) extended to four domains. The system can then be solved using the time-stepping method in (5.11).

6.4 Numerical Solutions for a Two-Asset European Put Option

In the following we present numerical results for the European put option with two underlying uncorrelated assets, (3.15), (3.16c), (6.1). The case of two uncorrelated assets is not likely in practice, however, it is an interesting case for studying the properties of spectral approximation. The parameters used in the numerical experiment are shown in Table 6.1.

Parameter	Value
r	0.05
σ_1	0.4
σ_2	0.4
K	100
T	0.5
$S_{\max}$	200

Table 6.1: Parameter values for the European put option with two underlying assets.

The Legendre Galerkin method coupled with the Crank-Nicolson method have been implemented with domain decomposition and the choice of subdomains is shown in Figure 6.1. The square domain is split into four along the strike price $K = 100$ of each dimension. The corresponding distribution of nodes is shown in Figure 6.2 when the polynomial degree of each subdomain Ω_i is $N_i = 4$ for $i = 1, 2, 3, 4$. As in the one-dimensional case we denote by N the sum of N_i's, i.e. $N = \sum_i N_i$. In addition, let us define $N_\circ$ to be the total number of nodes associated with a sum of polynomial degrees N. In the two-dimensional problem, more degrees of freedom are required for a certain polynomial order than in the one-dimensional case. In the following, the polynomial degree N_i is equally chosen on each subdomain. This gives $N = 4N_i$ and $N_\circ = (2N_i + 1)^2$.

The chosen domain partitioning reduces the computational time of the method as four of the blocks in the matrix system (5.15) can be assembled simultaneously. However, due to the shape of the payoff

function shown in Figure 6.3, this might not be an optimal partition of the domain. Considering the diagonal region of rapid change in the payoff function, a promising alternative would be to cluster more nodes along this diagonal.

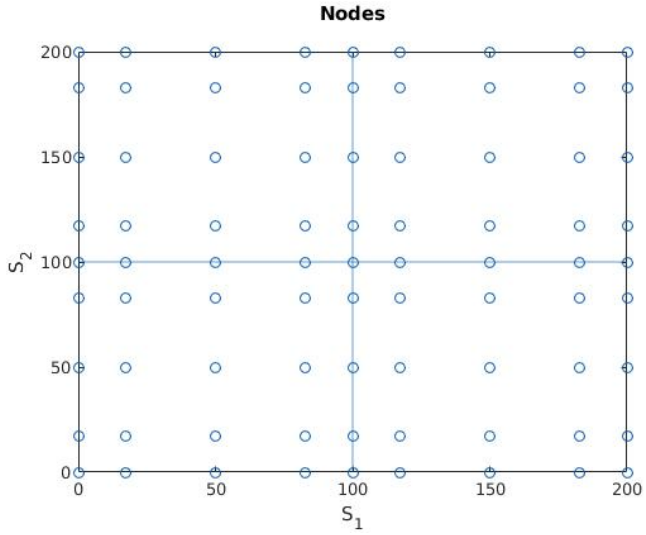

Figure 6.2: Distribution of the nodes when the polynomial degree of each subdomain Ω_i is $N_i = 4$ for $i = 1, 2, 3, 4$. The total number of nodes is $N_\circ = 81$.

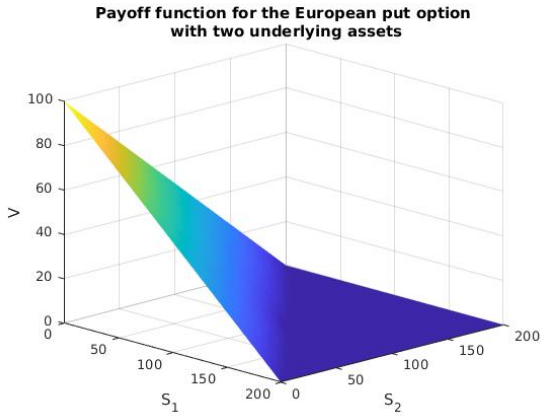

Figure 6.3: The payoff function for the European put option with two underlying assets.

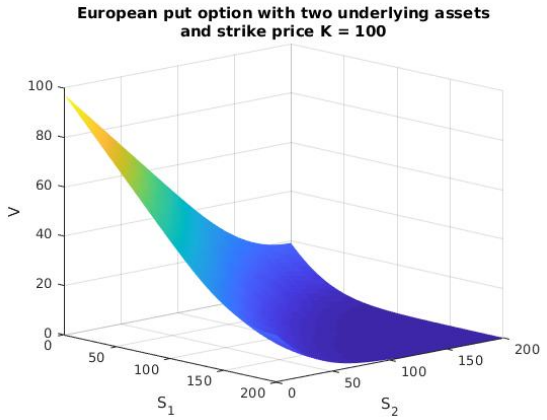

Figure 6.4: The reference solution for the European put option with two underlying assets, computed with $N = 120$.

As a reference solution for the multi-asset European pricing problem, the solution is computed with $N = 120$. This corresponds to the polynomial degree $N_i = 30$ on each subdomain Ω_i, $i = 1, 2, 3, 4$ and $N_\circ = 3721$. The solution is shown in Figure 6.4.

The solution of the problem obtained with $N = 8$, $N = 12$ and $N = 16$ is shown in Figure 6.5, Figure 6.6 and Figure 6.7, respectively. The solutions have been expanded through (6.14). For $N = 8$, the solution exhibits a slight oscillatory behaviour. For $N = 12$ and $N = 16$ the oscillatory behaviour is gone and the two solutions look inseparable already for these choices of polynomial orders.

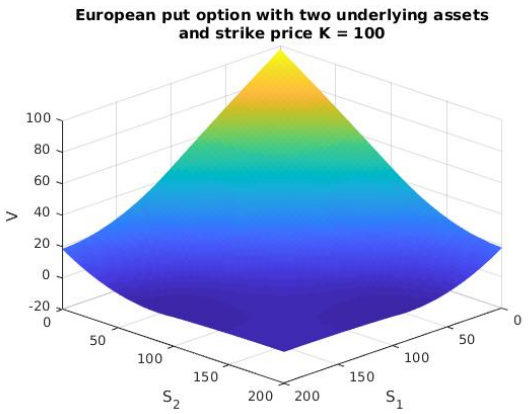

Figure 6.5: The solution of the two-asset pricing problem with $N = 8$.

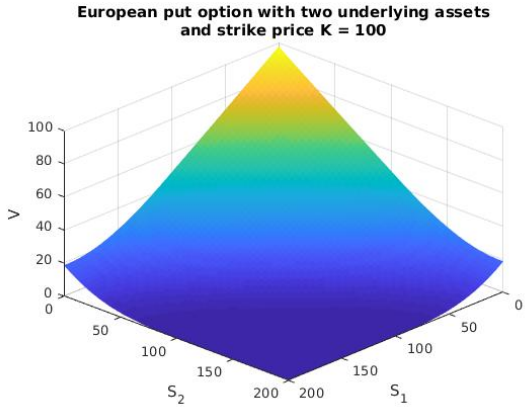

Figure 6.6: The solution of the two-asset pricing problem with $N = 12$.

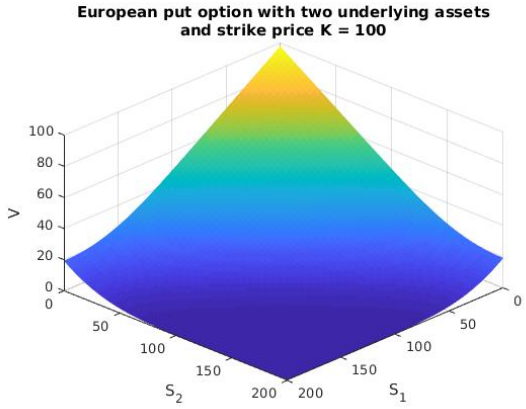

Figure 6.7: The solution of the two-asset pricing problem with $N = 16$.

In order to study the approximation error we use the norm defined in (6.10) to measure the difference between the approximate solution and the reference solution. The option price V in $\mathbf{S} = (K, K)$ and the errors related to increasing polynomial orders N_i are shown in Table 6.2.

The convergence of the method is shown in Figure 6.8. We observe a convergence rate of approximately fourth order. The method clearly outperforms the second order convergence of standard finite difference methods for option pricing. However, we do not observe the spectral convergence obtained for the single-asset European option. As shown in Table 6.2, the polynomial order $N_i = 24$ (corresponding to $N = 3N_i = 72$ in the single-asset case) yields an error of order 10^{-5} while an error of order 10^{-9} was obtained in the single asset problem, as shown in Table 5.2.

N_i	$N_\circ$	$V(K,K)$	$\|V_{\text{ref}} - V^N\|_{\tilde{L}^2}$
2	25	7.054850	9.445e-01
4	81	6.247754	6.739e-02
6	169	6.638205	5.502e-03
8	289	6.693073	2.957e-03
12	625	6.734036	5.872e-04
16	1089	6.748220	1.640e-04
20	1681	6.754756	3.515e-05
24	2401	6.758302	2.112e-05

Table 6.2: The option price V in $\mathbf{S} = (K, K)$ and the error measured with the approximated L^2-norm for different values of the polynomial degree N_i and the total number of nodes $N_\circ$.

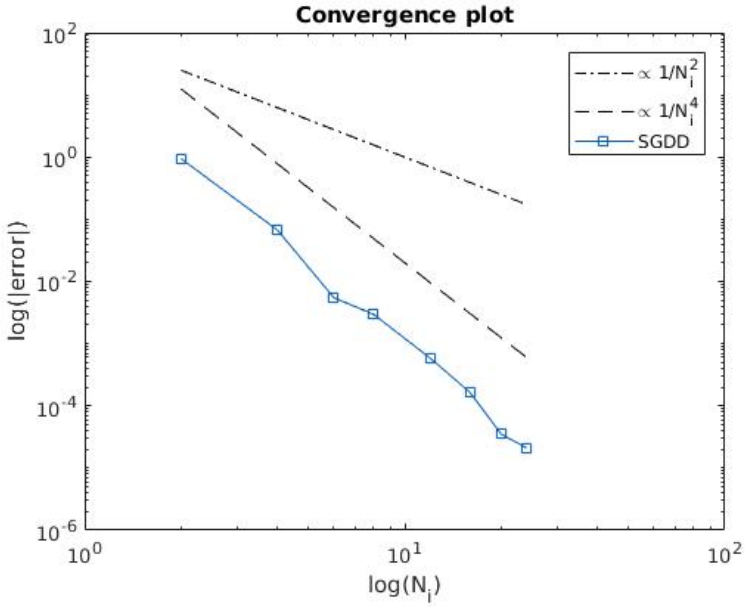

Figure 6.8: Log-log plot showing the convergence of the method with domain decomposition for N_i varying from 2 to 24. SGDD refers to Spectral Galerkin with domain decomposition.

The error corresponding to some of the choices of N_i used in the convergence test is shown in Figure 6.9. It is clear that the dominating error is localized along the diagonal of rapid change in the payoff function. However, the error has a faster rate of decay around the centre of the domain in $\mathbf{S} = (K, K)$. Here, nodes are clustered together due to the distribution of nodes following from the particular domain decomposition. These results indicate that spectral convergence may be obtained with a more clever choice of domain decomposition which increases the density of nodes along the region of rapid change in the payoff function.

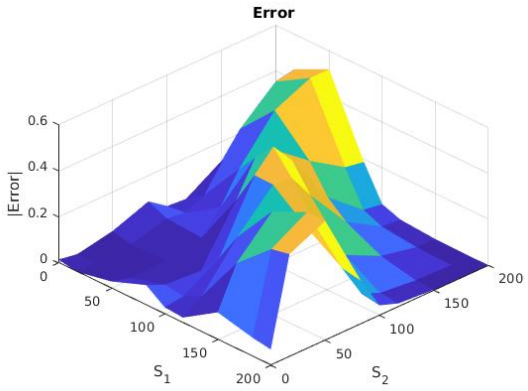

(a) Error between the numerical solution and the reference solution for $N_i = 4$.

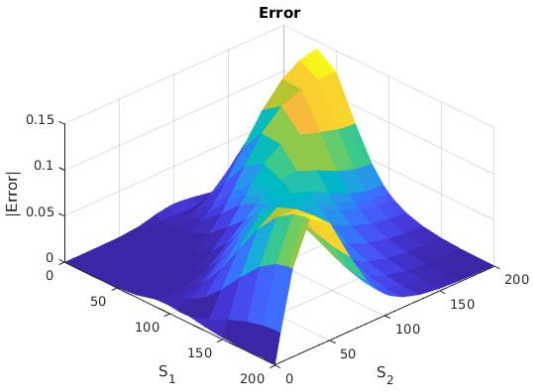

(b) Error between the numerical solution and the reference solution for $N_i = 8$.

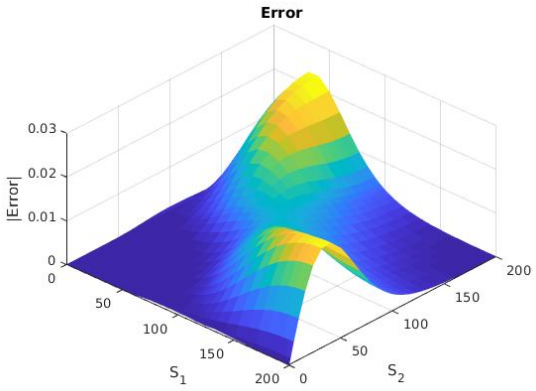

(c) Error between the numerical solution and the reference solution for $N_i = 16$.

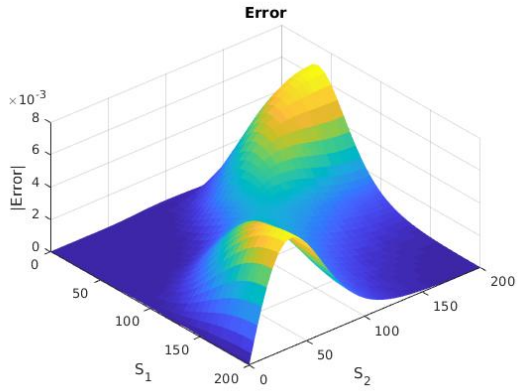

(d) Error between the numerical solution and the reference solution for $N_i = 24$.

Figure 6.9: Error between the numerical solution and the reference solution for different values of the polynomial order N_i.

Chapter 7

Analysis of the Numerical Scheme for European Options

We consider the one-dimensional Black–Scholes equation for a European option, (3.6). In the the following it will be convenient to substitute the time variable t with $T - t$. This gives a forward parabolic equation: for $S \geq 0$ and $t \in (0, T]$,

$$\begin{aligned} &\frac{\partial V(S,t)}{\partial t} - \frac{1}{2}\sigma^2 S^2 \frac{\partial^2 V(S,t)}{\partial S^2} - rS\frac{\partial V(S,t)}{\partial S} + rV(S,t) = 0, \\ &V(S,0) = V_\circ(S), \end{aligned} \tag{7.1}$$

where $V_\circ$ is the payoff function.

The following analysis is based on a similar analysis in chapter two of [2]. We consider the equation (7.1) on the domain $I = (0, \bar{S})$, with $\bar{S}$ a positive constant $\bar{S} > K$ and assume that we have homogeneous Dirichlet boundary conditions. Let us introduce the function space

$$W = \left\{ v \in L^2(I) \;\middle|\; x\frac{dv}{dx} \in L^2(I) = 0 \right\},$$

where the derivative must be understood in the sense of distributions on I. Furthermore, let

$$W_0 = \left\{ v \in W(I) \;\middle|\; v(\bar{S}) = 0 \right\}. \tag{7.2}$$

We equip the space W_0 with the inner product

$$(v,w)_W = (v,w)_{L^2} + \left(x\frac{dv}{dx}, x\frac{dw}{dx}\right)_{L^2},$$

and the norm

$$\|v\|_W = (v,v)_W^{1/2},$$

and one can easily check that W_0 is a Hilbert space.

If $v \in W_0$ the following Poincaré inequality holds, (see [2], Section 2.3.1),

$$\|v\|_{L^2(I)} \;\leq\; 2\left\|x\frac{dv}{dx}\right\|_{L^2(I)}.$$

Using the above inequality one can show that the seminorm $|v|_{W(I)} = \left\|x\frac{dv}{dx}\right\|_{L^2(I)}$ is equivalent to the full norm $\|v\|_{W(I)}$.

Multiplying equation (7.1) by a test function $\psi \in W_0$ and integrating over S, using integration by parts on the term with a second derivative, we obtain

$$\int_I \frac{\partial V}{\partial t}\psi\, dS + (\sigma^2 - r)\int_I S\frac{\partial V}{\partial S}\psi\, dS + \frac{1}{2}\sigma^2\int_I S^2\frac{\partial V}{\partial S}\frac{d\psi}{dS}\, dS + r\int_I V\psi\, dS - \frac{1}{2}\sigma^2\bar{S}^2\frac{\partial V}{\partial S}\left(\bar{S}\right)\psi(\bar{S}) = 0.$$

Since $\psi(\bar{S}) = 0$ we arrive at

$$\int_I \frac{\partial V}{\partial t}\psi\, dS + (\sigma^2 - r)\int_I S\frac{\partial V}{\partial S}\psi\, dS + \frac{1}{2}\sigma^2\int_I S^2\frac{\partial V}{\partial S}\frac{d\psi}{dS}\, dS + r\int_I V\psi\, dS = 0.$$

The bilinear form associated with this weak formulation is

$$a(V,\psi) = (\sigma^2 - r)\int_I S\frac{\partial V}{\partial S}\psi\, dS + \frac{1}{2}\sigma^2\int_I S^2\frac{\partial V}{\partial S}\frac{d\psi}{dS}\, dS + r\int_I V\psi\, dS.$$

The constants σ and r are assumed to satisfy $r \geq 0$ and $\sigma > 0$.

The Galerkin scheme for problem (7.1) is defined by

$$\begin{cases} V^N \in C^1\left([0,+\infty); W_N\right) \\ \left(\frac{\partial V^N}{\partial t}(t), \psi\right) + a(V^N, \psi) \;=\; 0 \quad \text{for all } \psi \in W_N,\ t > 0, \\ V^N(0) = V_\circ^N, \end{cases} \tag{7.3}$$

where $V_\circ^N$ is an approximation of the payoff function and W_N is a finite dimensional subspace of W_0 defined by $W_N = \mathbb{P}_N(0, \bar{S}) \cap W_0$.

In order to show stability for the Galerkin approximation, we start out by showing that the bilinear form is continuous on $W_0 \times W_0$:

$$\begin{aligned} |a(u,v)| \;&\leq |\sigma^2 - r| \int_I \left| S\frac{\partial u}{\partial S} v \right| dS + \frac{1}{2}\sigma^2 \int_I \left| S^2 \frac{\partial u}{\partial S}\frac{dv}{dS} \right| dS + r\int_I |uv|\, dS \\ &\leq |\sigma^2 - r| \left\| S\frac{\partial u}{\partial S} \right\|_{L^2(I)} \|v\|_{L^2(I)} + \frac{1}{2}\sigma^2 \left\| S\frac{\partial u}{\partial S} \right\|_{L^2(I)} \left\| S\frac{\partial v}{\partial S} \right\|_{L^2(I)} \\ &\quad + r\,\|u\|_{L^2(I)}\,\|v\|_{L^2(I)} \\ &\leq 2|\sigma^2 - r||u|_{W(I)}|v|_{W(I)} + \frac{1}{2}\sigma^2 |u|_{W(I)}|v|_{W(I)} + 4r|u|_{W(I)}|v|_{W(I)} \\ &\leq \mu |u|_{W(I)}|v|_{W(I)}, \end{aligned}$$

with $\mu = (\, 2|\sigma^2 - r| + \sigma^2/2 + 4r\,)$.

Furthermore, a bilinear form is said to be weakly coercive if there exists $\lambda \geq 0$ and $\alpha > 0$ such that

$$a(v,v) + \lambda \|v\|_{L^2}^2 \geq \alpha \|v\|_W^2,$$

yielding for $\lambda = 0$ the standard definition of coercivity.

Considering $a(v,v)$ for $v \in W_0$, we see that

$$
\begin{aligned}
a(v,v) &= (\sigma^2 - r)\int_I S\frac{\partial v}{\partial S} v\, dS + \frac{1}{2}\sigma^2 \int_I \left(S\frac{\partial v}{\partial S}\right)^2 dS + r\int_I v^2\, dS \\
&= \frac{(\sigma^2 - r)}{2}\int_I S\frac{\partial v^2}{\partial S}\, dS + \frac{1}{2}\sigma^2 \int_I \left(S\frac{\partial v}{\partial S}\right)^2 dS + r\int_I v^2\, dS \\
&= -\frac{(\sigma^2 - r)}{2}\int_I v^2\, dS + \frac{1}{2}\sigma^2 \int_I \left(S\frac{\partial v}{\partial S}\right)^2 dS + r\int_I v^2\, dS \\
&= -\frac{(\sigma^2 - 3r)}{2}\int_I v^2\, dS + \frac{1}{2}\sigma^2 \int_I \left(S\frac{\partial v}{\partial S}\right)^2 dS \\
&= -\frac{(\sigma^2 - 3r)}{2}\|v\|^2_{L^2(I)} + \frac{1}{2}\sigma^2 \left\|S\frac{\partial v}{\partial S}\right\|^2_{L^2(I)} \\
&\geq -\max\left(\frac{\sigma^2 - 3r}{2}, 0\right)\|v\|^2_{L^2(I)} + \frac{1}{2}\sigma^2 |v|^2_{W(I)}.
\end{aligned}
$$

Hence the bilinear form is weakly coercive with $\lambda = \max\left({}^{(\sigma^2 - 3r)}/_2, 0\right)$ and $\alpha = {}^{\sigma^2}/_2$.

Regarding the existence of a solution to problem (7.3) we make the following remark:

Remark 3 *Normally, continuity and weak coercivity of a bilinear form leads to the existence of a unique solution, see [28], Section 11.1.1. Our case is however not quite standard due to the weighted W-norm which makes a boundary condition in $S = 0$ unnecessary. Still, we expect there to exist a unique solution to the problem* (7.3)*.*

Now, we show that the following a priori estimate holds for the solution to problem (7.3):

Theorem 7.0.1 *The solution to problem* (7.3) *satisfies the stability estimate*

$$
e^{-2\lambda t}\|V^N(t)\|^2_{L^2(I)} + 2\alpha\int_0^t e^{-2\lambda s}|V^N(s)|^2_{W(I)} ds \;\leq\; \|V^N_\circ\|^2_{L^2(I)}.
$$

Proof. First, let us notice that if we introduce $V^N_\lambda(S,t) := e^{-\lambda t}V^N(S,t)$, where $V^N(S,t)$ is the solution to (7.3) the new unknown V^N_λ solves

$$
\left(\frac{\partial V^N_\lambda}{\partial t}(t), v\right) + a_\lambda(V^N_\lambda, v) \;=\; 0 \quad \text{for all } v \in W_N,\; t > 0,
$$

where $a_\lambda(u,w) = a(u,w) + \lambda(u,w)$ is coercive. We consider this problem solved by V^N_λ.

A weak formulation must hold for each $v \in W_N$, hence we can set the test function equal to the solution itself, $v = V^N_\lambda(S,t) = e^{-\lambda t}V^N(S,t)$, with t being given. Then the weak formulation

becomes

$$0 = \int_I \frac{\partial V_\lambda^N}{\partial t} V_\lambda^N \, dS + a_\lambda(V_\lambda^N, V_\lambda^N) \geq \frac{1}{2} \int_I \frac{\partial}{\partial t} \left(e^{-2\lambda t} (V^N)^2 \right) \, dS + \alpha e^{-2\lambda t} |V^N|^2_{W(I)}$$
$$= \frac{1}{2} \frac{d}{dt} \left(e^{-2\lambda t} \|V^N\|^2_{L^2(I)} \right) + \alpha e^{-2\lambda t} |V^N|^2_{W(I)}.$$

By integrating in time we obtain, for all $t > 0$

$$e^{-2\lambda t} \|V^N(t)\|^2_{L^2(I)} + 2\alpha \int_0^t e^{-2\lambda s} |V^N(s)|^2_{W(I)} ds \leq \|V_\circ^N\|^2_{L^2(I)}.$$

□

Concerning the convergence of the spectral approximation, let us introduce a projection operator, for all $N > 0$,

$$R_N : \mathcal{W}_0 \longrightarrow W_N, \tag{7.4}$$

such that for $N \to \infty$,

$$\|R_N u - u\|_W \longrightarrow 0 \quad \text{for all} \quad u \in \mathcal{W}_0. \tag{7.5}$$

Writing $a(u, v) = (\mathcal{L}u, v)$, the space $\mathcal{W}_0$ is a dense subspace $\mathcal{W}_0 \subseteq D_B(\mathcal{L})$ where $D(\mathcal{L})$ is the domain of $\mathcal{L}$ and $D_B(\mathcal{L})$ is defined as $D_B(\mathcal{L}) = \{w \in D(\mathcal{L}) \mid w \text{ satisfies the given boundary conditions}\}$.

Before stating a result on convergence, let us also define the dual norm

$$\|w\|_{W^*} = \sup_{\substack{v \in W \\ v \neq 0}} \frac{(w, v)}{|v|_W}, \tag{7.6}$$

for any function $w \in W_0$.

Then, we have the following result

Theorem 7.0.2 *Let R_N be the projection operator in* (7.4) *and let $e(t) = R_N V(t) - V^N(t)$.*

Then, the error function $e(t)$ satisfies for all $t > 0$ the error bound

$$e^{-2\lambda t}\|e(t)\|^2_{L^2(I)} + \alpha \int_0^t e^{-2\lambda s}|e(s)|^2_{W(I)}ds \ \leq$$
$$\|e(0)\|^2_{L^2(I)} + C\left(\int_0^t e^{-2\lambda s}\|(V_t - R_N V_t)(s)\|^2_{W^*(I)}ds + \int_0^t e^{-2\lambda s}|(V - R_N V)(s)|^2_{W(I)}ds\right).$$

Since $V - V^N = V - R_N V + e$ and therefore $\|V - V^N\| \leq \|e\| + \|V - R_N V\|$, Theorem 7.0.2 gives an error bound that can be used to evaluate convergence of the approximate solution. We can conclude from Theorem 7.0.2 that the approximation is convergent if each term on the right-hand side tends to 0 as $N \to \infty$ for V, V_t, and $V_\circ$ regular enough. This is true if (7.5) holds uniformly in t for functions $u(t)$ and $u_t(t)$ in a suitable class. This property is guaranteed by approximation results given in e.g [13], chapter 5.

Proof of Theorem 7.0.2. As in the proof of Theorem 7.0.1, let us consider $V^N_\lambda(S,t) := e^{-\lambda t}V^N(S,t)$, where $V^N(S,t)$ is the solution to (7.3). Then, the unknown $V^N_\lambda(S,t)$ solves

$$\left(\frac{\partial V^N_\lambda}{\partial t}(t), v\right) + a_\lambda\left(V^N_\lambda, v\right) = 0 \quad \text{for all } v \in W_N,\ t > 0, \tag{7.7}$$

where a_λ is continuous with continuity constant $C' = \mu + 4\lambda$ and coercive with coercivity constant α. As the true solution V_λ satisfies (7.7), we also have

$$\left(\frac{\partial V_\lambda}{\partial t}(t), v\right) + a_\lambda\left(V_\lambda, v\right) = 0 \quad \text{for all } v \in W_N,\ t > 0.$$

Inserting the error function $e(t) = R_N V_\lambda(t) - V^N_\lambda(t)$ into the left hand side of equation (7.7) gives

$$\left(\frac{\partial}{\partial t}e(t), e(t)\right) + a_\lambda\left(e(t), e(t)\right) =$$
$$\left(\frac{\partial}{\partial t}\left(R_N V_\lambda(t) - V^N_\lambda(t)\right), e(t)\right) + a_\lambda\left(R_N V_\lambda(t) - V^N_\lambda(t), e(t)\right) =$$
$$\left(\frac{\partial}{\partial t}\left(R_N V_\lambda(t)\right), e(t)\right) + a_\lambda\left(R_N V_\lambda(t), e(t)\right) - \left(\frac{\partial}{\partial t}V^N_\lambda(t), e(t)\right) - a_\lambda\left(V^N_\lambda(t), e(t)\right) =$$
$$\left(\frac{\partial}{\partial t}(R_N V_\lambda(t)), e(t)\right) + a_\lambda\left(R_N V_\lambda(t), e(t)\right) - \left(\frac{\partial}{\partial t}V_\lambda(t), e(t)\right) - a_\lambda\left(V_\lambda(t), e(t)\right) =$$
$$\left(R_N\frac{\partial}{\partial t}V_\lambda(t) - \frac{\partial}{\partial t}V_\lambda(t), e(t)\right) + a_\lambda\left(R_N V_\lambda(t) - V_\lambda(t), e(t)\right).$$

Then, using the coercivity of a_λ which gives

$$\alpha|e(t)|^2_{W(I)} \leq a_\lambda(e(t), e(t)),$$

we see that the error function $e(t)$ satisfies

$$\frac{1}{2}\frac{d}{dt}\|e\|^2_{L^2(I)} + \alpha|e|^2_{W(I)} \leq |(V_{\lambda t} - R_N V_{\lambda t}, e) + a_\lambda(V_\lambda - R_N V_\lambda, e)|.$$

Then, using definition (7.6) and the continuity of a_λ, it follows that

$$|(V_{\lambda t} - R_N V_{\lambda t}, e) + a_\lambda(V_\lambda - R_N V_\lambda, e)| \ \leq \ \|V_{\lambda t} - R_N V_{\lambda t}\|_{W^*(I)}|e|_{W(I)} + C'|V_\lambda - R_N V_\lambda|_{W(I)}|e|_{W(I)}.$$

Therefore, we have

$$\frac{1}{2}\frac{d}{dt}\|e(t)\|^2_{L^2(I)} + \alpha|e(t)|^2_{W(I)} \ \leq \ C\left(\|V_{\lambda t} - R_N V_{\lambda t}\|_{W^*(I)} + |V_\lambda - R_N V_\lambda|_{W(I)}\right)|e|_{W(I)},$$

where $C = \max(1, C')$ and by integrating in time we get, for all $t > 0$

$$\begin{aligned}
&\|e(t)\|^2_{L^2(I)} + \alpha \int_0^t |e(s)|^2_{W(I)} ds \ \leq \\
&\|e(0)\|^2_{L^2(I)} + C\left(\int_0^t \|(V_{\lambda t} - R_N V_{\lambda t})(s)\|^2_{W^*(I)} ds + \int_0^t |(V_\lambda - R_N V_\lambda)(s)|^2_{W(I)} ds\right).
\end{aligned}$$

Inserting $e^{-\lambda t}V^N(S,t)$ for $V^N_\lambda(S,t)$ and $e^{-\lambda t}V(S,t)$ for $V_\lambda(S,t)$ gives the result stated in Theorem 7.0.2.

□

To get an optimal error estimate, $R_N V$ is usually chosen as the best approximation of V in W_N with respect to the norm $|\cdot|_W$, or as an element in W_N that asymptotically behaves like the best approximation in this norm, namely

$$|V - R_N V|_W \leq C \inf_{v \in W_N} |V - v|_W,$$

for a constant C not depending on N.

In the above analysis we have considered a Galerkin approximation, while the scheme (5.10) is a Galerkin scheme with numerical integration. Under similar requirements as the ones above, a scheme with numerical integration can be analyzed in a similar manner (see [13], sect. 6.5.1).

The analysis of the scheme for the two-dimensional case is not included here, but would be similar to the one-dimensional case.

Chapter 8

The Single-Asset American Pricing Problem

8.1 The Variational Inequality

In the following we seek to determine the value $V(S,t)$ of an American option. For the American option, early exercise is permitted at any time prior to expiration. Since this type of option gives more rights to the owner than the European style option, its price should be higher. Consider, as earlier for the European pricing problem, an asset with price S which follows the stochastic process

$$dS_t = S_t(\mu dt + \sigma dX_t),$$

where μ is the drift rate, σ is the volatility and dX_t is the increment of a standard Brownian motion process. Following the introduction in Chapter 6 of [35], there exists a probability $\mathbb{P}*$ under which the value of the asset is a martingale. It is possible to prove that under this probability, the value of the American option with payoff $V_\circ$ and expiration time T is

$$V(S_t,t) = \sup_{\tau \in \mathcal{T}_{t,T}} \mathbb{E}^* \left(e^{-\int_t^\tau r(s)ds} V_\circ(S_\tau) \middle| F_t \right),$$

where $\mathcal{T}_{t,T}$ denotes the set of stopping times with values in $[t,T]$, (see [20]). It can be proven that

$V(S,t)$ is also the solution to the variational form of the following set of inequalities:

$$\frac{\partial V}{\partial t} + \frac{\sigma^2}{2} S^2 \frac{\partial^2 V}{\partial S^2} + rS\frac{\partial V}{\partial S} - rV \leq 0 \quad \text{in } \mathbb{R}_+ \times [0,T), \tag{8.1a}$$

$$V - V_\circ \geq 0 \quad \text{in } \mathbb{R}_+ \times [0,T), \tag{8.1b}$$

$$\left(\frac{\partial V}{\partial t} + \frac{\sigma^2}{2} S^2 \frac{\partial^2 V}{\partial S^2} + rS\frac{\partial V}{\partial S} - rV \right) (V - V_\circ) = 0 \quad \text{in } \mathbb{R}_+ \times [0,T), \tag{8.1c}$$

with final data

$$V|_{t=T} = V_\circ.$$

The proof can be found in [20].

In the following we will consider the theory of a vanilla put, having the payoff function (3.7). To a large extent, these results hold also for more general functions [2].

Two major methodologies for determining the value of an American option is the quasi-variational inequality formulation as described in [4, 5] and a free boundary problem formulation as in [21, 33]. In the following we propose another formulation based on the penalty method. With the penalty formulation, we avoid the difficulties associated with the side constraints that need to be fulfilled in the quasi-variational inequality formulation and there is no free boundary that needs to be determined, as in the free boundary formulation. This approach allows for the use of numerical algorithms that are easier to implement than those based on the quasi-variational inequality formulation and the free boundary problem formulation.

8.2 The Penalty Method

In order to solve the American pricing problem (8.1) numerically we propose a penalization method which provides an approximation to the American option value. We present a nonsmooth Newton iteration to solve the resulting penalized problem.

The idea of the penalty method is to replace problem (8.1) by the nonlinear partial differential equation

$$\frac{\partial V_\epsilon}{\partial t} - \left(\frac{\sigma^2}{2} S^2 \frac{\partial^2 V_\epsilon}{\partial S^2} + rS \frac{\partial V_\epsilon}{\partial S} - rV_\epsilon \right) + \frac{1}{\epsilon} \left[V_\circ - V_\epsilon \right]^+ = 0, \tag{8.2}$$

where $1/\epsilon$ is the penalty parameter. The nonlinear term $1/\epsilon \left[V_\circ - V_\epsilon \right]^+$ is used to penalize the positive part of $V_\circ - V_\epsilon$.

For bounded $\mathcal{L}V_\epsilon$, where $\mathcal{L}$ denotes the Black-Scholes differential operator, and $1/\epsilon$ sufficiently large, $[V_\circ - V_\epsilon]^+ \approx 0$, so that (8.1b) is satisfied within a tolerance depending on $1/\epsilon$ [34]. It has been shown in [4] that the rate of convergence of the piecewise linear penalty approach (8.2) is of order $\mathcal{O}(\epsilon^{1/2})$.

Using this approach we obtain the penalized problem

$$\begin{cases} \frac{\partial V_\epsilon}{\partial t} - \left(\frac{\sigma^2}{2} S^2 \frac{\partial^2 V_\epsilon}{\partial S^2} + rS \frac{\partial V_\epsilon}{\partial S} - rV_\epsilon \right) + \frac{1}{\epsilon} \left[V_\circ - V_\epsilon \right]^+ = 0, \\ V_\epsilon|_{t=T} = V_\circ. \end{cases} \tag{8.3}$$

We augment the problem (8.3) with the boundary conditions (3.8a),(3.9). Then the weak formulation of the problem reads

$$\begin{cases} \text{For } \ t \in (0,T) \text{ a.e., find } \ V_\epsilon(t) \in W \ \text{ such that} \\ \frac{d}{dt} \left(V_\epsilon(t), \psi \right) + a(V_\epsilon(t), \psi) + \frac{1}{\epsilon} ([V_\circ - V_\epsilon]^+, \psi) = 0 \quad \text{for all} \quad \psi \in W, \\ V_\epsilon|_{t=T} = V_\circ, \end{cases} \tag{8.4}$$

for W defined in (7.2) and with $(\cdot, \cdot)$ and $a(\cdot, \cdot)$ given in (5.4).

A proof of the existence of a unique solution in W to (8.4) can be found in [34].

One of the advantages of the penalty method is that the associated algorithm has finite termination, i.e for an iterate sufficiently close to the solution, the algorithm terminates in one iteration. This is particularly advantageous in American option pricing where we have an excellent initial guess from the solution in the previous timestep. Finite termination also implies that the number of iterations required for convergence is insensitive to the size of the penalty term, up until machine precision. Furthermore, if the penalized problem is solved using Newton iteration, the iteration is globally convergent when using full Newton steps [18].

Another advantage of the penalty method is that a single technique can be used for one dimensional

or multi-dimensional problems. Hence this is a suitable method for extending the American pricing problem to higher dimensions. This could be relevant for designing an efficient method for pricing American options on baskets which is still an interesting open problem [2].

8.3 A Legendre Galerkin Scheme with Numerical Integration and Domain Decomposition

We now semi-discretize the problem (8.4), localized on $(0, S_{\max})$, with the Legendre Galerkin method used earlier for the European option.

In the case of European options we initially observed lower order convergence attributed to the non-smooth payoff function. As a remedy for this, we apply domain decomposition also in the case of American options, since we are dealing with the same initial data and in addition have discontinuous second derivatives across the early exercise boundary. For simplicity, theory will be presented for the choice of two subdomains.

Let us split the domain $\Omega = (0, S_{\max})$ into the two subdomains

$$\Omega_1 = (0, K), \;\; \Omega_2 = (K, S_{\max}).$$

As trial and test functions we take again the Lagrange polynomials based on the Legendre Gauss-Lobatto nodes defined in (5.1) and denote by N_i the polynomial order in Ω_i, $i = 1, 2$.

Upon setting $V_\epsilon^{(i)} = V_{\epsilon|\Omega_i}$, and for $(\cdot,\cdot)_{\Omega_i}$ and $a_i(\cdot,\cdot)$ defined as in (5.16), the two-domain formulation of (8.4) is

$$\begin{cases} \text{For } \; t \in (0,T) \text{ a.e., find } \; V_\epsilon^{(i)}(t) \in W \;\; \text{such that} \\ \frac{d}{dt}\left(V_\epsilon^{(i)}(t), \psi_j^{(i)}\right)_{\Omega_i} + a_i\left(V_\epsilon^{(i)}(t), \psi_j^{(i)}\right) + \frac{1}{\epsilon}\left([V_\circ - V_\epsilon^{(i)}(t)]^+, \psi_j^{(i)}\right)_{\Omega_i} = 0, \\ V^{(i)}(0) = V_{\circ|\Omega_i}, \qquad j = 0, ..., N_i, \quad i = 1, 2, \end{cases} \tag{8.5}$$

accompanied by the following interface conditions

$$\begin{cases} V_\epsilon^{(1)}(S) = V_\epsilon^{(2)}(S) \\ \frac{\partial V_\epsilon^{(1)}}{\partial n}(S) = -\frac{\partial V_\epsilon^{(2)}}{\partial n}(S), \qquad S \in \partial\Omega_1 \cap \partial\Omega_2. \end{cases} \tag{8.6}$$

We set $V_\epsilon^{(i)} = V_{\epsilon|\Omega_i}$, and search for a spectral approximation $V_\epsilon^{(N,i)}$ to the solution $V_\epsilon^{(i)}$ of the problem (8.5), (8.6) in the form

$$V_\epsilon^{N,(i)} = \sum_{k=0}^{N_i} V_{\epsilon,k}^{(i)}(t)\psi_k^{(i)}(x), \quad x \in \Omega_i, \qquad i = 1, 2, \tag{8.7}$$

where $\psi_k^{(i)}$ are the trial functions associated with the nodes in $\overline{\Omega}_i$.

The interpolated penalty term is given by

$$\begin{aligned} \pi_\epsilon^{N,(i)}\left(V_\epsilon^{N,(i)}\right) &= \sum_{k=0}^{N_i} \pi_\epsilon\left(V_\epsilon^{N,(i)}\right)(x_k, t)\psi_k^{(i)}(x) \\ &= \frac{1}{\epsilon}\sum_{k=0}^{N_i}\left[V_{\circ,k} - V_{\epsilon,k}^{(i)}(t)\right]^+ \psi_k^{(i)}(x), \quad x \in \Omega_i, \quad i = 1, 2, \end{aligned} \tag{8.8}$$

where $V_{\circ,k}$ is the initial value in node k.

After mapping each subdomain to the reference domain $\hat{\Omega} = (-1, 1)$ through the linear transformation in (5.7) and inserting the approximations $V_\epsilon^{N,(i)}$ in (8.7) and $\pi_\epsilon^{N,(i)}\left(V_\epsilon^{N,(i)}\right)$ in (8.8) we obtain the numerical scheme

$$\begin{aligned} &J_1 \int_{\hat{\Omega}} \frac{dV}{dt}^{N,(1)} \psi_j^{(1)} d\xi + \frac{1}{2J_1}\sigma^2 K^2 \frac{\partial V^{N,(1)}}{\partial \xi}\psi_j^{(1)}(K) \\ &- (\sigma^2 - r)\int_{\hat{\Omega}} S(\xi)\frac{\partial V^{N,(1)}}{\partial \xi}\psi_j^{(1)} d\xi - \frac{1}{2J_1}\sigma^2 \int_{\hat{\Omega}} S^2(\xi)\frac{\partial V^{N,(1)}}{\partial \xi}\frac{d\psi_j^{(1)}}{d\xi} d\xi \\ &- rJ_1 \int_{\hat{\Omega}} V^{N,(1)}\psi_j^{(1)} d\xi + J_1 \int_{\hat{\Omega}} \pi_\epsilon^{N,(1)}(V_\epsilon^{N,(1)})(t)\psi_j^{(1)} d\xi = 0, \quad \xi \in \hat{\Omega}, \quad j = 0, ..., N_1 \end{aligned}$$

$$\begin{aligned} &J_2 \int_{\hat{\Omega}} \frac{dV}{dt}^{N,(2)} \psi_j^{(2)} d\xi - \frac{1}{2J_2}\sigma^2 K^2 \frac{\partial V^{N,(2)}}{\partial \xi}\psi_j^{(2)}(K) \\ &- (\sigma^2 - r)\int_{\hat{\Omega}} S(\xi)\frac{\partial V^{N,(2)}}{\partial \xi}\psi_j^{(2)} d\xi - \frac{1}{2J_2}\sigma^2 \int_{\hat{\Omega}} S^2(\xi)\frac{\partial V^{N,(2)}}{\partial \xi}\frac{d\psi_j^{(2)}}{d\xi} d\xi \\ &- rJ_2 \int_{\hat{\Omega}} V^{N,(2)}\psi_j^{(2)} d\xi + J_2 \int_{\hat{\Omega}} \pi_\epsilon^{N,(2)}(V_\epsilon^{N,(2)})(t)\psi_j^{(2)} d\xi = 0, \quad \xi \in \hat{\Omega}, \quad j = 0, ..., N_2, \end{aligned}$$

where J_i is the Jacobian of the transformation associated with $\Omega_i, i = 1, 2$.

If we now apply the Gauss-Lobatto quadrature formula (5.9) in order to evaluate the integrals, we arrive at the scheme

$$
\begin{aligned}
&J_1 \sum_{k=0}^{N} w_k \left(\frac{dV^{N,(1)}}{dt} \psi_j^{(1)} \right)(\xi_k) + \frac{1}{2J_1}\sigma^2 K^2 \frac{\partial V^{N,(1)}}{\partial \xi}\psi_j^{(1)}(1) \\
&- (\sigma^2 - r) \sum_{k=0}^{N} w_k \left(S \frac{\partial V^{N,(1)}}{\partial \xi}\psi_j^{(1)} \right)(\xi_k) - \frac{1}{2J_1}\sigma^2 \sum_{k=0}^{N} w_k \left(S^2 \frac{\partial V^{N,(1)}}{\partial \xi}\frac{d\psi_j^{(1)}}{d\xi} \right)(\xi_k) \\
&- rJ_1 \sum_{k=0}^{N} w_k \left(V^{N,(1)}\psi_j^{(1)} \right)(\xi_k) + J_1 \sum_{k=0}^{N} w_k \left(\pi_\epsilon^{N,(1)} \left(V^{N,(1)} \right) \psi_j^{(1)} \right)(\xi_k) = 0, \\
&\qquad\qquad \xi \in \hat{\Omega}, \;\; j = 0, ..., N_1
\end{aligned}
$$

$$
\begin{aligned}
&J_2 \sum_{k=0}^{N} w_k \left(\frac{dV^{N,(2)}}{dt} \psi_j^{(2)} \right)(\xi_k) - \frac{1}{2J_2}\sigma^2 K^2 \frac{\partial V^{N,(2)}}{\partial \xi}\psi_j^{(2)}(-1) \\
&- (\sigma^2 - r) \sum_{k=0}^{N} w_k \left(S \frac{\partial V^{N,(2)}}{\partial \xi}\psi_j^{(2)} \right)(\xi_k) - \frac{1}{2J_2}\sigma^2 \sum_{k=0}^{N} w_k \left(S^2 \frac{\partial V^{N,(2)}}{\partial \xi}\frac{d\psi_j^{(2)}}{d\xi} \right)(\xi_k) \\
&- rJ_2 \sum_{k=0}^{N} w_k \left(V^{N,(2)}\psi_j^{(2)} \right)(\xi_k) + J_2 \sum_{k=0}^{N} w_k \left(\pi_\epsilon^{N,(2)} \left(V^{N,(2)} \right) \psi_j^{(2)} \right)(\xi_k) = 0, \\
&\qquad\qquad \xi \in \hat{\Omega}, \;\; j = 0, ..., N_2,
\end{aligned}
$$

where ξ_k and w_k are the Legendre Gauss-Lobatto nodes and weights, respectively.

After incorporating the interface conditions (8.6) into these equations we can write the system in the form

$$M\dot{V} + AV + M\Pi_\epsilon(V - V_\circ) = 0, \tag{8.9}$$

with M and A set up as in (5.13) and (5.14), respectively, and Π_ϵ is the diagonal matrix with entries

$$[\Pi_\epsilon]_{ii} = \begin{cases} \frac{1}{\epsilon}, & V_i < V_{\circ,i} \\ 0, & \text{otherwise.} \end{cases} \tag{8.10}$$

In total, we have a system of $N + 1$ algebraic equations, when setting $N = N_1 + N_2$.

We can now find a numerical solution by implementing an appropriate solver for the nonlinear system

(8.9). One possibility is to discretize the system in time using a two-level implicit time-stepping method and then use Newton iteration to solve the resulting nonlinear discrete equations.

If we define, based on (8.10)

$$[\Pi_\epsilon(V^{n+1})]_{ii} = \begin{cases} \frac{1}{\epsilon}, & V_i^{n+1} < V_{\circ,i} \\ 0, & \text{otherwise,} \end{cases}$$

and denote $\Pi_{\epsilon,n+1} \equiv \Pi_\epsilon(V^{n+1})$, then applying the time-stepping method (5.11) with splitting parameter $\theta \in [1/2, 1]$ to (8.9) gives the fully discrete system

$$\begin{aligned} &M(V^{n+1} - V^n) + \Delta t A[\theta V^{n+1} + (1-\theta)V^n] + \Delta t \theta M \Pi_{\epsilon,n+1}(V^{n+1} - V_\circ) \\ &+ \Delta t(1-\theta) M \Pi_{\epsilon,n}(V^n - V_\circ) = 0, \end{aligned} \tag{8.11}$$

where $\Delta t = t^{n+1} - t^n$.

8.4 Penalty Iteration

Let us define

$$\left(\bar{\Pi}_{\epsilon,n+1}\right)_i = \begin{cases} \frac{1}{\epsilon}, & V_i^{n+1} < V_{\circ,i} \\ 0, & \text{otherwise,} \end{cases}$$

and let the derivative of the penalty term, required in the Newton iteration, be given by

$$\frac{\partial \left(\bar{\Pi}_{\epsilon,n+1}\right)_i \left(V_{\circ,i} - V_i^{n+1}\right)}{\partial V_i^{n+1}} = \begin{cases} -\frac{1}{\epsilon}, & V_i^{n+1} < V_{\circ,i} \\ 0, & \text{otherwise.} \end{cases}$$

This is one particular choice of a member of the generalized Jacobian of the system (8.11). Based on this we can present the following algorithm constructed from a generalized Newton iteration applied to (8.11) [18].

Let $\left(V^{n+1}\right)^k$ be the k^{th} estimate for V^{n+1}. For notational convenience, we set $\Pi_{\epsilon,n+1}^k \equiv \Pi_\epsilon\left(\left(V^{n+1}\right)^k\right)$ and $V^k \equiv \left(V^{n+1}\right)^k$. If we take as initial guess $V^0 = V^n$, then

For $k = 0, ...$ until convergence

$$\left[M + \Delta t \left(A\theta + \theta M \Pi^k_{\epsilon,n+1}\right)\right] V^{k+1} = \left[M - \Delta t \left(A(1-\theta) - (1-\theta) M \Pi^k_{\epsilon,n}\right)\right] V^n$$

$$+ \Delta t \left[\theta M \Pi^k_{\epsilon,n+1} + (1-\theta) M \Pi^k_{\epsilon,n}\right] V_\circ$$

$$\text{if} \quad \left[\max_i \frac{\left|\left(V_i^{n+1}\right)^{k+1} - \left(V_i^{n+1}\right)^k\right|}{\max\left(1, \left|\left(V_i^{n+1}\right)^{k+1}\right|\right)} < tol\right] \quad \text{or} \quad \left[\Pi_\epsilon^{k+1} = \Pi_\epsilon^k\right] \quad \text{quit}$$

End For,

where tol is some specified tolerance.

An alternative for solving the nonlinear system (8.9) is to use MATLAB's ODE solver `ode15s` [1], which provides an efficient solver for stiff differential equations. This method have been used in the numerical experiments presented in the following section.

8.5 Numerical Solutions for a Single-Asset American Put Option

Here we present results from solving the American vanilla pricing problem (8.1), (3.7), (3.9) using the penalty Legendre Galerkin method with numerical integration and domain decomposition. The penalty term is set to $1/\epsilon = 10^8$. After the spatial discretization, the resulting ODE has been solved using MATLAB's ODE solver `ode15s`, for which documentation can be found in B.1. The results are shown for the final timestep.

The choice of parameters are shown in Table 8.1.

Parameter	Value
r	0.05
σ	0.2
K	10
T	0.25
$S_{\max}$	60

Table 8.1: Parameter values for the American put option.

The domain decomposition has been implemented with four subdomains, $\Omega_1 = (0, A)$, $\Omega_2 = (A, K)$, $\Omega_3 = (K, B)$, $\Omega_4 = (B, S_{\text{max}})$, where A and B have been chosen in order to optimize the convergence rate. The values $A = 8.68$ and $B = 22$ have been used in all experiments in this section. The value of A corresponds to the point of early exercise at the final timestep. As earlier we let N denote the sum of polynomial degrees on each subdomain, i.e. $N = \sum_i N_i$, $i = 1, 2, 3, 4$. The distribution of the nodes for $N_i = 7$ on each subdomain Ω_i is shown in Figure 8.1. All the following results have been obtained with equal N_i's on each subdomain.

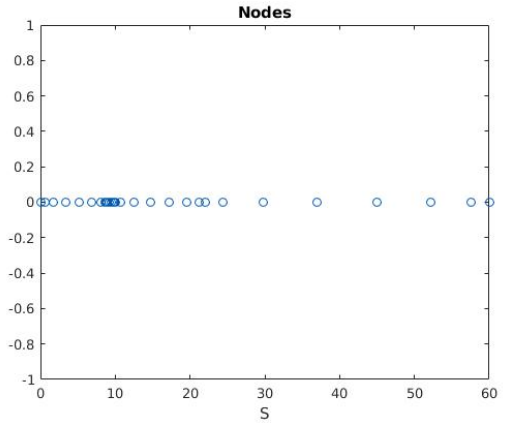

(a) Distribution of the nodes along the S-axis.

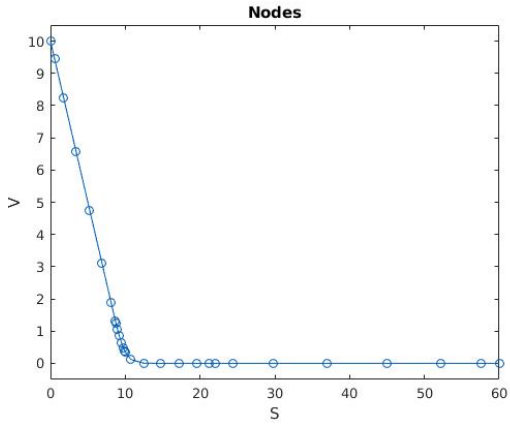

(b) Distribution of option values V corresponding to the nodes in (a).

Figure 8.1: Distribution of nodes in the case $N_i = 7$ for $i = 1, 2, 3, 4$. In (a) the distribution of the nodes is shown along the S-axis while (b) shows the location of each calculated option value V based on these nodes.

The optimal exercise boundary for the American pricing problem with the given parameters is shown in Figure 8.2.

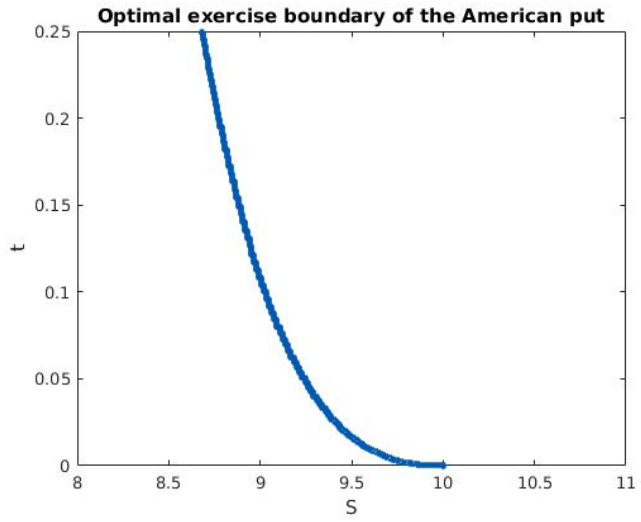

Figure 8.2: The optimal exercise boundary for an American put with parameters as in Table 8.1.

Since the American pricing problem (8.1), (3.7), (3.9) does not admit a viable exact solution we compare numerical results to a reference solution of fine resolution computed with $N = 560$, corresponding to the polynomial degree $N_i = 140$ on each subdomain Ω_i, $i = 1, 2, 3, 4$. The reference solution is shown in Figure 8.3.

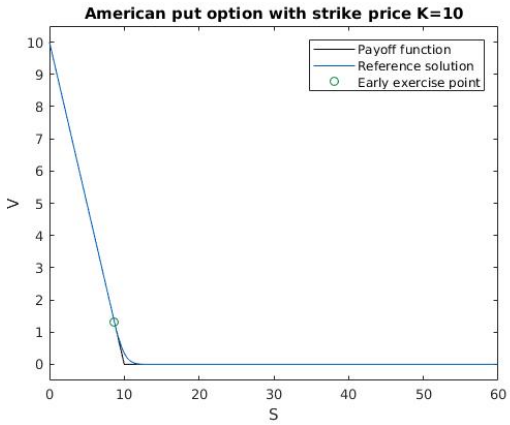

(a) Option price solution with $N = 560$.

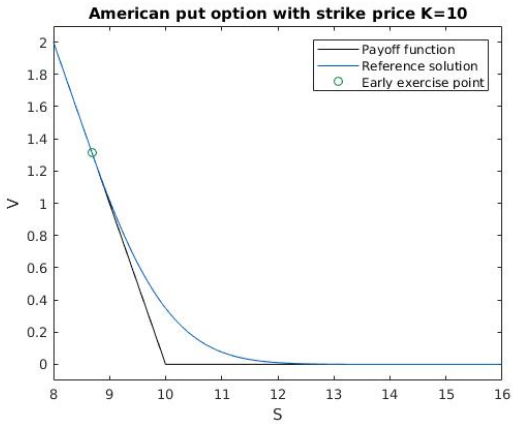

(b) An enlarged image of the case in (a) around the region of rapid change.

Figure 8.3: Option price solution used as a reference solution in the numerical experiments.

Numerical solutions for different values of N are shown in Figure 8.4. Setting $N = 16$ gives the results in Figures 8.4a and 8.4b. The option price for the whole domain $\Omega = (0, S_{\text{max}})$ is shown to the left and the right hand side shows an enlarged image of the option price around the strike price K. The numerical solution exhibits oscillatory behaviour and deviates significantly from the exact solution. Increasing N slightly to $N = 20$ gives the results shown in Figures 8.4c and 8.4d. For this value of N, the oscillatory behaviour is less prominent. Results for $N = 28$, found in Figures 8.4e and 8.4f, shows a solution very similar to the reference solution.

N_i	$V(K)$	$\|V_{\text{ref}} - V^N\|_{\tilde{L}^2}$
2	0.28458938	5.504e-02
4	0.39164045	1.403e-02
8	0.34883499	8.778e-04
16	0.34801996	1.744e-05
32	0.34798737	8.549e-07
64	0.34798545	1.238e-07
128	0.34798567	7.786e-09

Table 8.2: The option price V in $S = K$ and the error measured with the approximated L^2-norm for different values of $N_i, i = 1, 2, 3, 4$.

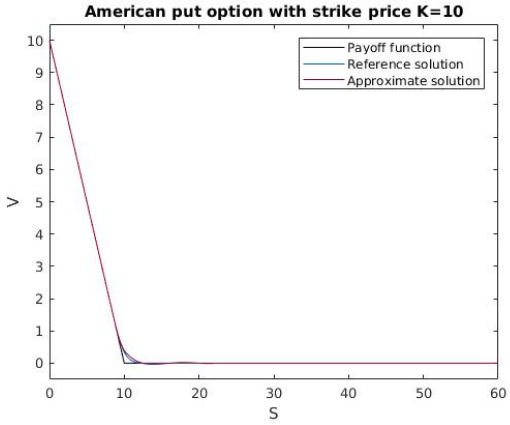

(a) Option price solution obtained with $N = 16$.

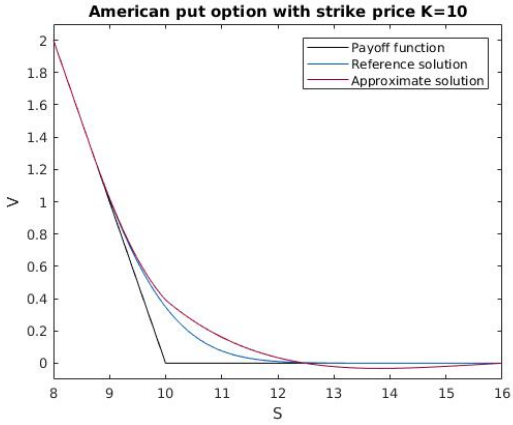

(b) An enlarged image of the case in (a) around the region of rapid change.

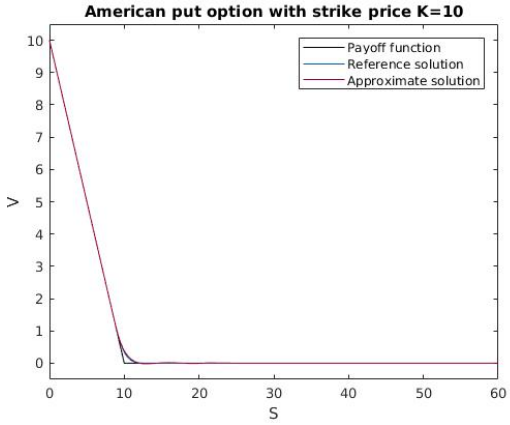

(c) Option price solution obtained with $N = 20$.

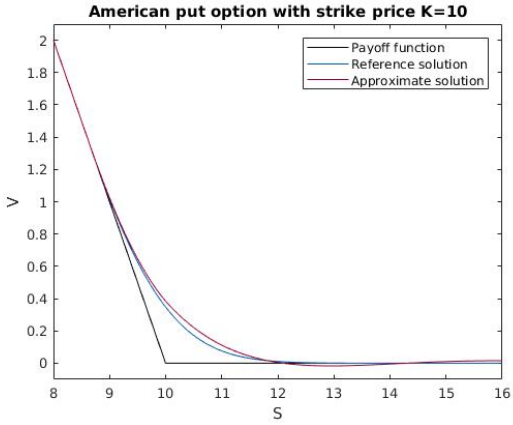

(d) An enlarged image of the case in (c) around the region of rapid change.

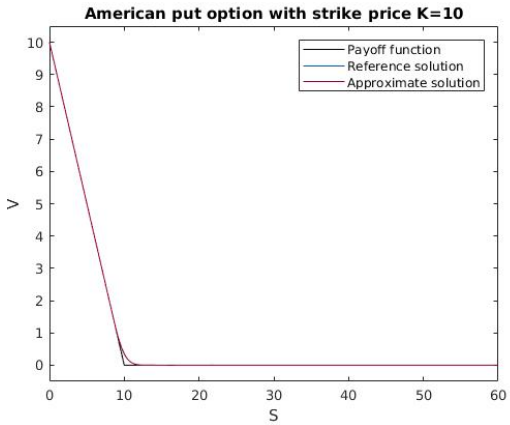

(e) Option price solution obtained with $N = 28$.

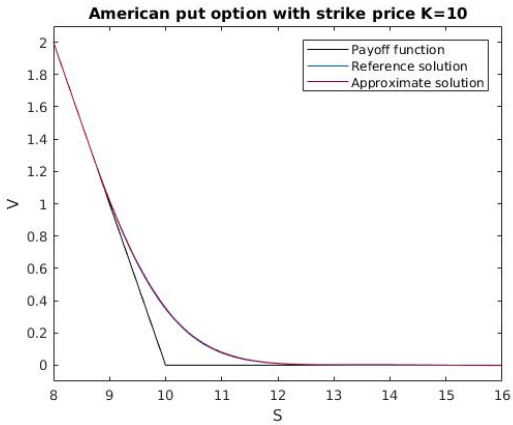

(f) An enlarged image of the case in (e) around the region of rapid change.

Figure 8.4: The solution of the American pricing problem for different values of N compared to a reference solution with $N = 560$.

In order to study the approximation error, the norm defined in (5.12) is used to measure the difference between the approximate solution and the reference solution. The option price V in $S = K$ and the errors related to increasing values of the polynomial order N_i are shown in Table 8.2.

Convergence of the method is shown in Figure 8.5. We observe a convergence rate of approximately fourth order. Spectral accuracy is not obtained, and it is clear that the error decays slower than in the case of single-asset European options. However, in terms of convergence rates, the method is superior to second order methods like standard finite differences.

The error for some of the values of N_i used in the convergence test is shown in Figure 8.6. The dominating error is located near the slope discontinuity of the payoff function in $S = K$ and at the point of early exercise. This is not surprising due to the non-smoothness of the payoff function in $S = K$ and the discontinuous second derivatives across the early exercise boundary of the American option value. An error is also associated with the subdomain interface in B. Based on the error plots, it seems possible to find a more optimal partitioning of the domain Ω that could further increase the rate of convergence. One possibility is to track the early exercise boundary through time and let this point be the interface of the first two subdomains. However, this would result in more complex computations. Another idea for improvement is to adapt the polynomial order in each subdomain such that the density of nodes on each side of the interface is more similar. It may also be advantageous to investigate a more sophisticated penalty formulation, since large values of the penalty parameter is known to cause computational problems in practice [16].

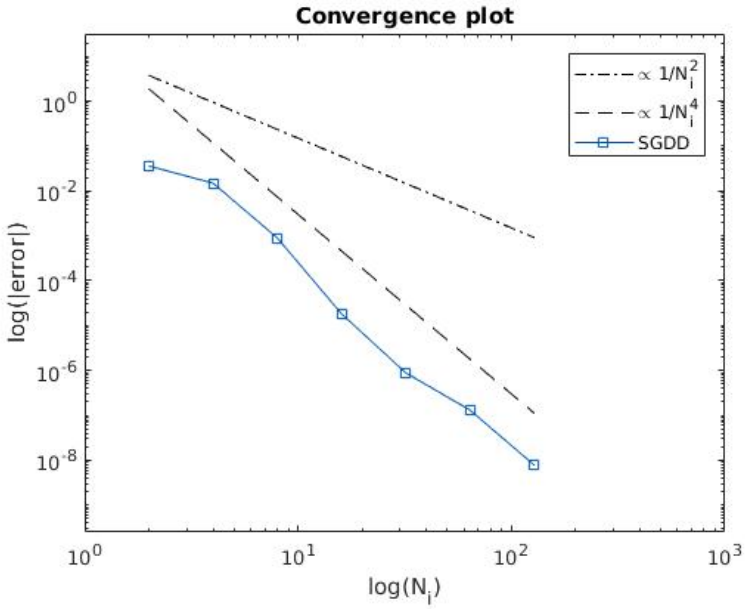

Figure 8.5: Log-log plot showing the convergence of the method with domain decomposition for N_i varying from 2 to 128. SGDD refers to Spectral Galerkin with domain decomposition.

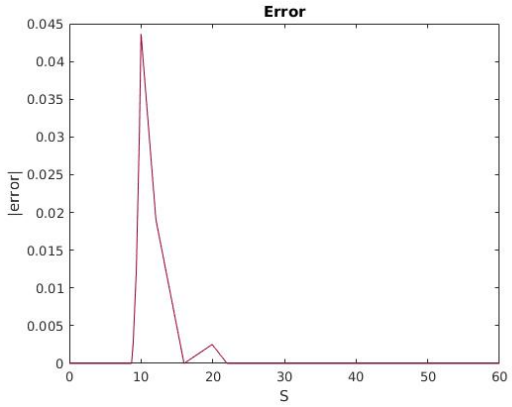

(a) Error between the numerical solution and the reference solution for $N_i = 4$.

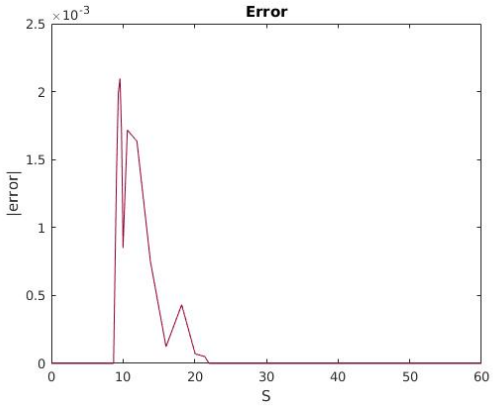

(b) Error between the numerical solution and the reference solution for $N_i = 8$.

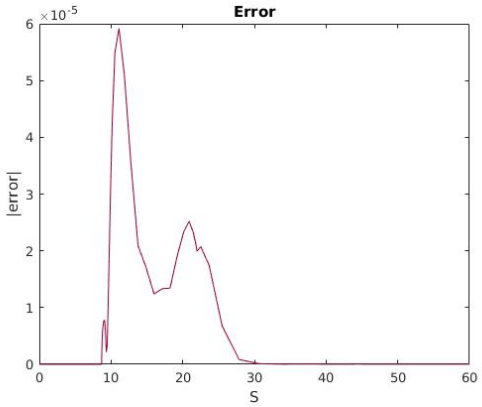

(c) Error between the numerical solution and the reference solution for $N_i = 16$.

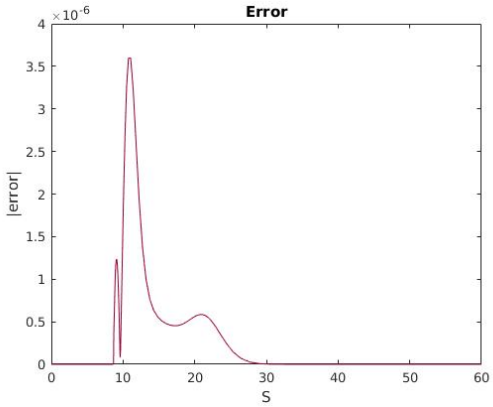

(d) Error between the numerical solution and the reference solution for $N_i = 32$.

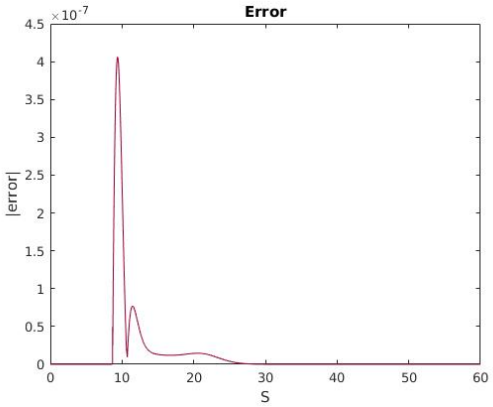

(e) Error between the numerical solution and the reference solution for $N_i = 64$.

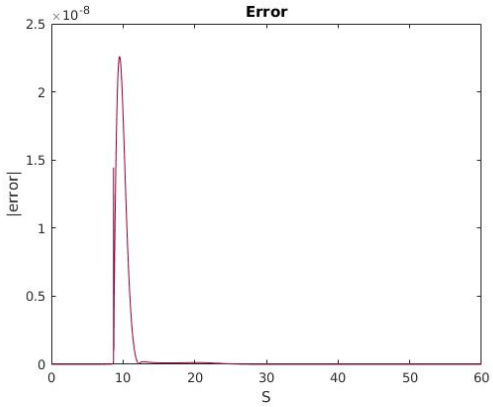

(f) Error between the numerical solution and the reference solution for $N_i = 128$.

Figure 8.6: Error between the numerical solution and the reference solution for different values of the polynomial order N_i.

Chapter 9

Conclusion

The aim of this thesis has been to develop spectral methods for option pricing in one and two dimensions under the Black-Scholes model. The work is motivated by interesting challenges existing in several option pricing problems. Legendre Galerkin schemes with numerical integration and domain decomposition has been derived for pricing European and American options. In the case of European vanilla options spectral convergence is obtained, providing evidence that the method is promising for option pricing problems. The implementation of domain decomposition proves to be an efficient remedy for eliminating low-order convergence due to non-smooth payoff functions.

For the two-asset European pricing problem, a convergence rate of fourth order is observed. The geometry of the problem combined with numerical results indicate that spectral convergence might be obtained with a more clever domain decomposition. For American vanilla options, the method has been implemented based on a penalty formulation. Also for this problem, fourth order convergence is observed. The error decays at a slower rate than in the case of single-asset European options. The slower convergence compared to single-asset European options may be due to the less smooth solution of American options and the more challenging geometry attributed to the optimal exercise boundary. Numerical results indicate that the convergence rate may be improved with a more optimal choice of subdomains in the domain decomposition method. In total, quite satisfactory results have been found for some basic standard and non-standard options. The conclusion is thus that the Legendre Galerkin method with numerical integration and domain decomposition is a very promising alternative for option pricing problems.

Chapter 10

Suggestions for Further Work

Numerical experiments for the two-asset European pricing problem shown in Section 6.4 and the American pricing problem shown in Section 8.5 both lack to provide fully satisfactory convergence results. Further work on the choice of subdomains in the domain decomposition method may be sufficient to restore spectral convergence for these option pricing problems. For the two-dimensional European problem, it is tempting to investigate a coordinate transformation that rotates the grid 45°, in order to cluster nodes on the diagonal of rapid change of the payoff function.

As mentioned in Section 8.2, the given piecewise linear penalty approach used for the American pricing problem has been shown to be of order $\mathcal{O}(\epsilon^{1/2})$. This convergence rate requires the penalty parameter $1/\epsilon$ to be sufficiently large in order to achieve a given accuracy of an approximate solution. However, large values of $1/\epsilon$ are known to cause computational issues in practice [16]. As an alternative, one may consider the power penalty method presented for option pricing by Wang et al. [34], which is shown to be of order $\mathcal{O}(\epsilon^{k/2})$. This allows for obtaining an accurate solution with a small penalty parameter.

It would further be interesting to extend the work beyond two dimensions in space. Derivative securities in financial markets often depend on a variety of underlying financial variables combined with early exercise features. Examples are American basket options with multiple underlying assets, American options on foreign currencies and convertible bonds. If spectral convergence is obtained, the method might outperform current methods for multi-asset option problems, like Monte Carlo methods.

In relation to the topic above, it would also be interesting to further investigate appropriate time differencing methods. High order convergence in time is necessary to make multidimensional applications

practical. The difficulty is again associated with the non-smooth payoff function and the discontinuous second derivatives across the early exercise boundary of the American option. Attempts to solve the PDE with standard high-order time discretization methods with a fixed time step generally encounters difficulties, as high-order fixed time step discretization schemes require the existence of higher order derivatives to realize high order convergence [24].

Further work could also be put into a thorough comparison study, comparing the method presented here to several other existing methods seen in the literature. If the Legendre-Galerkin spectral method can compete with other methods in terms of both accuracy and computational complexity, it could potentially be interesting in financial applications. In addition to comparing the method to fundamentally different methods, one could also compare it to other types of spectral methods such as the rational spectral collocation method discussed for options by Pindza [27].

Finally, another interesting task is to extend the analysis to establish the stability of the discretized American pricing problem and derive an error bound for the approximate solution.

Bibliography

[1] MathWorks ode15s. `https://www.mathworks.com/help/matlab/ref/ode15s.html`. Accessed: 2018-06-01.

[2] Achdou, Y. and Pironneau, O. (2005). *Computational Methods for Option Pricing*. SIAM, Society for Industrial and Applied Mathematics.

[3] Bensoussan, A. (1984). *On the Theory of Option Pricing*. Acta Appl. Math 2(2):139–158.

[4] Bensoussan, A. and Lions, J.-L. (1982). *Applications of Variational Inequalities in Stochastic Control*. North-Holland Publishing Co.

[5] Bensoussan, A. and Lions, J.-L. (1984). *Impulse Control and Quasivariational Inequalities*. Gauthier-Villars.

[6] Benth, F. (2001). *Matematisk finans Innføring i opsjonsteori med stokastisk analyse*. Universitetsforlaget.

[7] Benth, F. E., Karlsen, K. H., and Reikvam, K. (2003). *A Semilinear Black and Scholes Partial Differential Equation for Valuing American Options*. Finance Stochast. 7(3):277–298.

[8] Black, F. and Scholes, M. (1973). *The Pricing of Options and Corporate Liabilities*. J. Polit. Econ. 81, 637-659.

[9] Brennan, M. and Schwartz, E. (1978). *Finite Difference Methods and Jump Processes Arising in the Pricing of Contingent Claims: A Synthesis*. J. Financ. Quant. Analysis 13(3), 461–474.

[10] C. Canuto, M.Y. Hussaini, A. and Zang, T. (1988). *Spectral Methods in Fluid Dynamics*. Springer-Verlag, New York.

[11] Chan, T. F. and Mathew, T. P. (1994). *Domain Decomposition Algorithms*. Cambridge University Press.

[12] Chen, F., Shen, J., and Yu, H. (2011). *A New Spectral Element Method for Pricing European Options Under the Black–Scholes and Merton Jump Diffusion Models*. J Sci Comput (12) 52:499–518.

[13] Claudio, C., Hussaini, M., Quarteroni, A., and Zang, T. (2006). *Spectral Methods Fundamentals in Single Domains*. Springer.

[14] Cox, J., Ross, S., and Rubinstein, M. (1979). *Option Pricing: A Simplified Approach*. J. Financ. Econom. 7(2), 229–264.

[15] Flamouris, D. and Giamouridis, D. (2007). *Approximate Basket Option Valuation for a Simplified Jump Process*. Wiley Periodicals, Inc.

[16] Fletcher, R. (1987). *Practical Methods of Optimization*. Wiley and Sons, New York, NY.

[17] Fornberg, B. (1996). *A Practical Guide to Pseudospectral Methods*. Cambridge University Press.

[18] Forsyth, P. and Vetzal, K. (2001). *Quadratic Convergence for Valuing American Options Using a Penalty Method*. SIAM, Society for Industrial and Applied Mathematics.

[19] Greenberg, A. (2002). *Chebyshev Spectral Method for Singular Moving Boundary Problems with Application to Finance, PhD thesis*. California Institute Of Technology.

[20] Jaillet, P., Lamberton, D., and Lapeyre, B. (1990). *Variational Inequalities and the Pricing of American Options*. Acta Appl. Math., 21(3):263–289.

[21] Jr, H. P. M. (1965). *Appendix: A Free Boundary Problem for the Heat Equation Arising from a Problem in Mathematical Economics*. Indust. Manage. Rev. 6:32–39.

[22] Karatzas, I. (1988). *On the Pricing of American Options*. Appl. Math. Optim. 17(1):37–60.

[23] Karatzas, I. (1989). *Optimization Problems in the Theory of Continuous Trading*. SIAM J. Control Optim., 27(6):1221–1259.

[24] Kovalov, P., Linetsky, V., and Marcozzi, M. (2007). *Pricing Multi-Asset American Options: A Finite Element Method-of-Lines with Smooth Penalty*. J Sci Comput(7) 33: 209–237.

[25] Ngounda, E. and Patidar, K. C. (2015). *Limitations and Improvements of Standard Spectral Methods for Pricing Standard Options*. Int J Adv Eng Sci Appl Math 7(3):106–113.

[26] Nielsen, B., Skavhaug, O., and Tveito, A. (2002). *Penalty and Front-fixing Methods for the Numerical Solution of American Option Problems*. J. Comput. Financ. 5, 69–97.

[27] Pindza, E. (2012). *Robust Spectral Methods for Solving Option Pricing Problems*. Ph.D. thesis, University of the Western Cape.

[28] Quarteroni, A. and Valli, A. (1994). *Numerical Approximation of Partial Differential Equations*. Springer.

[29] Quarteroni, A. and Valli, A. (1999). *Domain Decomposition Methods for Partial Differential Equations*. Oxford University Press.

[30] Song, H., Zhang, R., and Tian, W. Y. (2014). *Spectral Method for the Black-Scholes Model of American Options Valuation*. J. Math. Study Vol. 47, No. 1, pp. 47-64.

[31] Tadmor, E. (1986). *The Exponential Accuracy of Fourier and Chebyshev Differencing Methods*. Journal of Numerical Analysis 23(1), 1-10.

[32] Tangman, D., Gopaul, A., and Bhuruth, M. (2007). *Exponential Time Integration and Chebychev Discretisation Schemes for Fast Pricing of Options*. Applied Numerical Mathematics 58 (8), 1309-1319.

[33] van Moerbeke, P. (1976). *On Optimal Stopping and Free Boundary Problems*. Arch. Rational Mech. Anal., 60(2):101–148.

[34] Wang, S., Yang, X. Q., and Teo, K. L. (2006). *Power Penalty Method for a Linear Complementarity Problem Arising from American Option Valuation*. Journal of Optimization Theory and Applications: Vol. 129, No. 2(6), pp. 227–254.

[35] Wilmott, P., Howison, S., and Dewynne, J. (1995). *The Mathematics of Financial Derivatives*. Cambridge University Press.

[36] Youbi, F., Pindza, E., and Maré, E. (2017). *A Comparative Study of Spectral Methods for Valuing Financial Options*. Applied Mathematics Information Sciences.

[37] Øksendal, B. (2003). *Stochastic Differential Equations An Introduction with Applications*. Springer.

Appendix

A Mathematics

A.1 Itô's Formula

Theorem A.1 The general Itô formula

Let

$$dX(t) = udt + vdB(t)$$

be an n-dimensional Itô process. Let $g(t,x) = (g_1(t,x), ..., g_p(t,x))$ be a C^2 map from $[0,\infty) \times \mathbb{R}^n$ into $\mathbb{R}^p$. Then the process

$$Y(t,\omega) = g(t, X(t))$$

is again an Itô process, whose component number k, Y_k is given by

$$dY_k = \frac{\partial g_k}{\partial t}(t,X)dt + \sum_i \frac{\partial g_k}{\partial x_i}(t,X)dX_i + \frac{1}{2}\sum_{i,j} \frac{\partial^2 g_k}{\partial x_i \partial x_j}(t,X)dX_i dX_j$$

where $dB_i dB_j = \delta_{ij}dt, dB_i dt = dt dB_i = 0$.

This formula can be found in [37], Section 4.2.

B Software and Implementation

B.1 MATLAB ODE Solver `ode15s`

The MATLAB solver `ode15s` is an ODE solver that solves stiff differential equations. It is a variable-step, variable-order solver based on the numerical differentiation formulas of orders one to five.

Description:

$[t, y]$ = ode15s(odefun, tspan, y_0), where tspan = $[t_0 \ t_f]$, integrates the system of differential equations $y' = f(t, y)$ from t_0 to t_f with initial conditions y_0.

For the full MATLAB documentation, see [1].